GENETIC MANIPULATION OF THE CELL WALL COMPOSITION OF SUGARCANE

Jan PI Bekker

Dissertation presented for the Degree of Doctor of Philosophy (Plant Biotechnology)
at the University of Stellenbosch

Supervisor: Prof. Jens Kossmann

March 2007

Declaration

I the undersigned hereby declare that the work contained in this dissertation is my own original work and that I have not previously in its entirety or in part submitted it at any university for a degree.

J Bekker

March 2007

ABSTRACT

In order to understand and manipulate carbon flux to sucrose one needs to consider not only its biosynthetic pathways, but also the competing sinks for carbon in various parts of the plant and at different stages of development. The cell wall and sucrose is known to be the major sinks for carbon in young and mature tissues of sugarcane. UDP-Glucose is a central metabolite in the synthesis of both sucrose and most of the cell wall polysaccharides (including cellulose, hemicellulose and pectic polymers) and manipulation of the flux into either of the cell wall components could therefore cause an increase of flux toward one or more of the competing sinks. In the present study UDP-Glucose dehydrogenase (UGD) activity was chosen for down regulation as it catalyzes the rate limiting step in the biosynthesis of the precursors of both hemicellulose and pectin, a major competing sink for assimilated carbon.

Transgenic sugarcane lines with repressed UGD activity showed significantly increased sucrose accumulation in all internodes which was highly correlated with reduced UGD activity. Sucrose phosphate synthase had increased activation which suggests an alteration in carbon flux toward sucrose.

The reduction of carbon flux through UGD was compensated for by an increase in the activity of the *myo*-inositol oxygenation pathway (MIOP), an alternative pathway for the synthesis of cell wall matrix precursors. The increased activity of the MIOP resulted in increased total uronic acids and pentoses in the cell wall. Total cell wall glucose was also increased which is a further indication of altered carbon metabolism.

OPSOMMING

Manipulasie van die fluks van koolstof na sukrose vereis kennis van beide die biosintetiese bane (source, bron) vir sukrose, sowel as die mededingende koolstof poele (sinks) in verskillende dele van die plant en tydens verskillende stadiums van ontwikkeling. Die selwand en sukrose is die hoof koolstof poele in jong en volwasse suikerriet weefsels. UDP-Glukose is ‘n sentrale metaboliet vir die sintese van beide sukrose en meeste van die selwand polisakkariede (insluitend sellulose, hemisellulose en pektiese polimere) en manipulasie van die fluks na een van die selwand komponente kan dus ‘n toename in die fluks na een of meer van die kompeterende poele veroorsaak. In hierdie studie word die aktiwiteit van UDP-Glukose dehidrogenase (UGD) afgereguleer om sodoende die fluks van koolstof na die sintese van hemisellulose en pektien, ‘n hoof poel vir geassimileerde koolstof, te verminder.

Transgeniese suikerriet met onderdrukte UGD aktiwiteit het beduidende toenames in sukrose akkumulasie in alle internodes getoon. Die toenames was hoogs gekorrelleer met die vermindering in UGD aktiwiteit. Sukrose fosfaat sintase (SPS) het ‘n toename in aktivering getoon wat verder dui op ‘n wysiging in koolstof fluks na sukrose.

Die afname in koolstof fluks deur UGD na hemisellulose en pektien was gekompenseer deur ‘n toename in aktiwiteit in die *mio*-inositol oksigenasie baan (MIOP), ‘n alternatiewe baan vir die sintese van selwand matriks voorgangers. Die toename in die aktiwiteit van die MIOP het ‘n toename in totale glukuronsuur sure en pentoses in die selwand tot gevolg gehad. Die totale selwand glukose en meer spesifiek die glukose in sellulose was ook verhoog wat ‘n verdere aanduiding is van ‘n wysiging in koolstof metabolisme in suikerriet met onderdrukte UGD aktiwiteit.

CONTENTS

ABBREVIATIONS

AIR	Alcohol insoluble residue
bp	Base-pairs
BSA	Bovine serum albumin
CeS	Cellulose synthase
DMSO	Dimethyl sulfoxide
DTT	Dithiotreitol
EDTA	Ethylenediaminetetra-acetate
EtOH	Ethanol
Fru-6-P	Fructose-6-phosphate
GC-MS	Gas chromatography/mass spectrometry
Glc-1-P	Glucose-1-phosphate
Glc-6-P	Glucose-6-phosphate
HEPES	4(2-hydroxyethyl)-1-piperazine-ethanesulphonic acid (buffer)
kDa	Kilo Dalton
MIOP	*Myo*-inositol oxygenation pathway
MIOX	*Myo*-inositol oxygenase
MS	Murashige and Skoog (media)
NAD^+	Nicotineamide adenine dinucleotide (oxidised)
NADH	Nicotineamide adenine dinucleotide (reduced)
$NADP^+$	Nicotinamide adenine dinucleotide phosphate (oxidised)
PCR	Polymerase chain reaction
PGI	Glucose-6-P isomerase
PGM	Phosphoglucomutase
P_i	Inorganic phosphate
PP_i	Inorganic pyrophosphate
RT	Room temperature (22 °C)
SDS	Sodium dodecyl sulphate
SPS	Sucrose phosphate synthase
SuSy	Sucrose synthase
Tris	2-amino-2-hydroxymethylpropane-1,3-diol (buffer)
UDP	Uridine diphosphate
UDP-Glc	UDP-D-Glucose
UGD	UDP-Glucose dehydrogenase
UGPase	UDP-Glucose pyrophosphorylase

GENETIC MANIPULATION OF THE CELL WALL COMPOSITION OF SUGARCANE

1.1 INTRODUCTION

Through selective cross-breeding practices, plant breeders have been able to increase the sucrose content of *Saccharum* spp. (sugarcane) consistently over the past 100 years[1]. However, over the last decade breeders have been unable to show significant increases in sucrose content using traditional plant breeding approaches and a plateau in synthesis/storage capacity seems to have been reached.

Sugarcane, cultivated mainly for its sucrose but also used for bio-ethanol production, the generation of electricity and other by-products, is one of the world's most important crop plants. Worldwide it is grown in tropical and subtropical areas in more than 80 countries on an estimated land area of over 18 million hectares. Due to its importance as a sucrose yielding crop, sugarcane has been targeted by the novel gene manipulation techniques used in the field of biotechnology to unravel the complexities of the metabolism of sucrose and related compounds and also to increase the sucrose synthesis/storage capacity *in vivo*. It is estimated that sugarcane could potentially store more than 25% sucrose per fresh weight which is almost double its present yield[1].

Various genetic manipulation strategies, discussed by Grof and Campbell (2001)[1] in their review of the topic, are currently being employed to redirect photosynthetically fixed carbon toward storage tissues and away from other sinks. Although the molecular tools for engineering high sucrose plants are available, and many targets for manipulation through overexpression or repression have been identified, this has not been achieved. Specific key target areas include sucrose synthesis in the leaf and stem, sucrose transport and the enzymes catalysing sucrose cleavage in stem tissues. An additional target area for manipulation is the plant cell wall as it represents a major carbon sink and is the most abundant reservoir of organic carbon in nature.

1.2 THE PLANT CELL WALL

The plant cell wall is the major determinant of the plant cell's shape and size. Furthermore, the cell wall also provides a defensive barrier, anchorage for the cytoskeleton, fulfils functions in cell recognition, growth and differentiation. The wall is highly organized and is made up of polysaccharides, proteins and various aromatic compounds which cross-link the polymers together to provide structural support. Cellulose fibers are embedded in a hydrogel

of matrix polysaccharides and small amounts of protein. The exact chemical composition of the wall varies considerably from species to species and between different plant organs in the same plant, but the basic design of the wall is consistent. The primary cell walls of dicots contain approximately 30% cellulose, 30% hemicellulose, 35% pectin with 1-5% protein (on a dry weight basis) compared to monocots that contain approximately 25% cellulose, 55% hemicellulose and 10% pectin[2,3].

UDP-D-Glucose (UDP-Glc) is the common precursor for most of the polymers found in the plant cell wall. In addition, UDP-Glc is also a substrate for sucrose synthesis. Together, the cell wall and sucrose represent the largest carbon sinks in plants. The central position occupied by UDP-Glc as a substrate for these sinks as well as the economic importance of its down-stream metabolic products makes the biosynthetic pathways leading from UDP-Glc a target for molecular manipulation. In the following section the various pathways leading from UDP-Glc are discussed with emphasis on its interconversion to UDP-Glucuronic acid (UDP-GlcA) by UDP-Glucose dehydrogenase (UGD).

1.3 NUCLEOTIDE SUGARS IN PLANTS

Nucleotide sugars are either synthesized from phosphorylated monosaccharides or through epimerization of precursor nucleotide sugars[4]. UDP-Glc, first isolated and studied by Leloir *et al.* (1951)[5], is a key metabolite of carbohydrate metabolism in both photosynthetic and non-photosynthetic plant tissues[6]. Nucleotide sugars represent between 10-25% of the total nucleotide pool of plants. Uridine nucleotides and in particular UDP-Glc predominate in the nucleotide-sugar pool of most plant tissues[7]. UDP-Glc contributes between 60-70% of total nucleotide-sugars followed by UDP-D-Galactose (UDP-Gal) making up 15-25%. In young and mature leaves, the main photosynthetic tissues, UDP-Glc is used for sucrose synthesis by sucrose phosphate synthase (SPS, EC 2.4.1.14) and sucrose synthase (SuSy, EC 2.4.1.13) to a lesser degree[8]. In addition, UDP-Glc is either used in cell wall synthesis (cellulose, callose, mixed β(1-3)(1-4)-glucans) or enters the interconversion pathways and is used indirectly as wall precursors. UDP-Glc also supplies the Glc units incorporated in glycolipids and glycoproteins[6].

1.4 PLANT UDP-GLC METABOLISM

UDP-Glc is a central metabolite in several anabolic pathways of plant carbohydrate metabolism. Not only is UDP-Glc the precursor for cellulose, callose and most of the cell wall matrix polysaccharides, but it also contributes the glucose-moiety for the glycosylation of small molecules and sucrose synthesis. The UDP-Glc 'pool' is maintained at three

intracellular sites namely the cytosol, the Golgi apparatus[9] and at the plasma membrane[10] where it is used in various biosynthetic activities.

Two major pathways exist for the synthesis of nucleotide sugars: (1) UDP-Glc is synthesized from uridine triphosphate (UTP) and glucose-1-phosphate (Glc-1-P) by UDP-Glc pyrophosphorylase (UGPase, EC 2.7.7.9) and (2) GDP-Man is synthesized from guanidine triphosphate (GTP) and mannose-1-phosphate (Man-1-P). An alternative and possibly more important pathway for the synthesis of UDP-Glc is catalyzed by SuSy.

Carbon can enter the hexose phosphate pool (glucose-6-phosphate (Glc-6-P), Glc-1-P and fructose-6-phosphate (Fru-6-P)) through gluconeogenesis by the phosphorylation of free hexoses, *via* the breakdown of starch or sucrose and through the reverse reactions of glycolysis on the triose phosphate products of photosynthesis[11] (Figure 1.1, p 9). The three constituent intermediates are kept in equilibrium by the actions of phosphoglucomutase (PGM) and glucose 6-P isomerase (PGI):

$$\text{Glc-1-P} \xleftrightarrow{PGM} \text{Glc-6-P} \xleftrightarrow{PGI} \text{Fru-6-P}$$

The carbon moieties of the hexose phosphate pool are used in the synthesis of sucrose, starch, cell wall polymers, in the pentose phosphate pathway and glycolysis (Figure 1.1, p 9).

Glc-1-P can enter and leave the hexose phosphate pool through UGPase. Many pyrophosphorylases have been demonstrated in plants, but UGPase which is responsible for the synthesis of UDP-Glc in both prokaryotic and eukaryotic systems, predominates (several 100- to several 1000-fold) over the pyrophosphorylases that catalyze the formation of GDP-Glc, TDP-Glc, ADP-Glc or GDP-Man. It is thought that the reason for this is the high levels of glucose-phosphates which are the primary products of photosynthesis. UGPase catalyzes the transfer of a uridyl unit between phosphate acceptors with the concomitant cleavage of inorganic pyrophosphate (PPi) in the nucleotide substrate[7]:

$$\text{UTP} + \text{Glc-1-P} \xleftrightarrow{UGPase} \text{UDP-Glc} + \text{PPi}$$

Although the UGPase reaction is known to be readily reversible *in vitro* it is assumed that because of the removal of PPi *in vivo* by an as yet elusive mechanism[11], intracellular levels of PPi does not reach levels high enough to favor the synthesis of Glc-1-P through the reverse reaction[7]. UDP-Glc exerts a strong inhibitory effect on UGPase with K_i-values of around 0.1 mM.

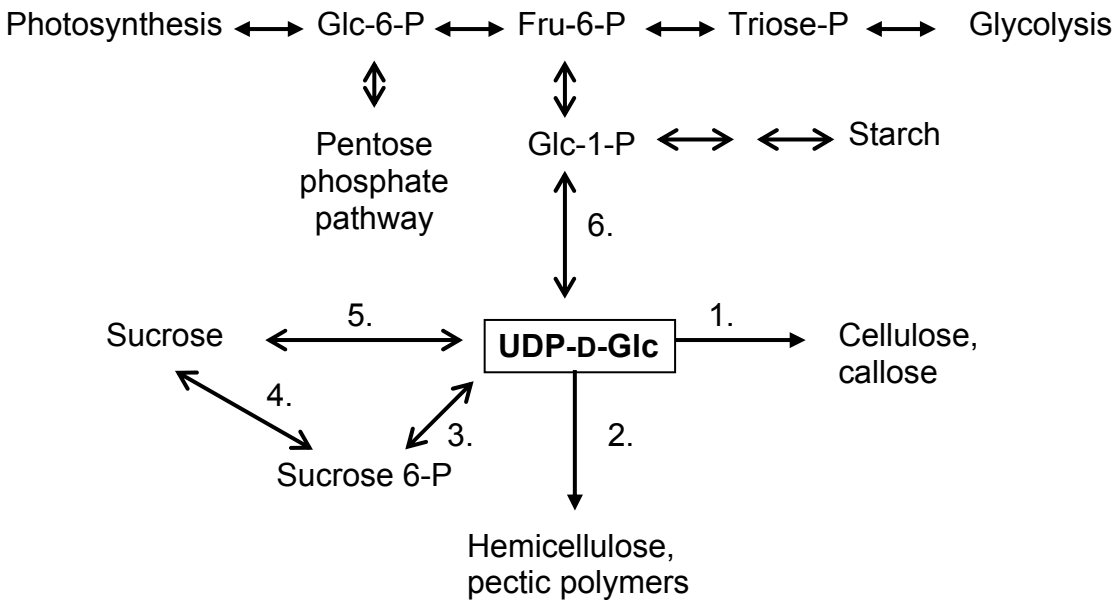

Figure 1.1: Central position of UDP-glucose in plant carbohydrate metabolism.

1. Cellulose/callose synthase; 2. UDP-Glucose dehydrogenase; 3. Sucrose phosphate synthase, 4. Sucrose phosphate phosphatase, 5. Sucrose synthase, 6. UDP-Glucose pyrophosphorylase.

The reactions that provide the major synthetic drains on the cytosolic UDP-Glc pool are those catalyzed by cellulose synthase (CeS), UGD, SPS and the many nucleotide sugar interconversion reactions.

1.4.1 CELLULOSE SYNTHESIS

It is has been suggested that cellulose, the major structural polysaccharide component of the plant cell wall, is the most abundant biopolymer on earth[12]. Additionally, most of the carbon fixed during photosynthesis is incorporated into cell wall polymers which make these structural elements of plants the most abundant source of biomass and energy[13]. All of the monosaccharides in cell wall polymers are derived from glucose. Many interconversion pathways exist for the various reactions needed to convert glucose into the ten major monosaccharides that occurs commonly in the cell wall of plants. The central point of departure for the interconversion reactions is UDP-Glc which is known to occur at three intracellular sites or 'pools', namely the cytosol, Golgi-apparatus and at the cell wall[9,10]. The cytosolic pool provides UDP-Glc for glycosylation of small molecules[14], nucleotide sugar interconversion reactions and through the reverse action of UGPase provides Glc-1-P for various metabolic pathways. Specific transporters for UDP-Glc were identified in isolated Golgi membrane vesicles of pea, providing evidence for the existence of a UDP-Glc pool inside the Golgi-apparatus[9]. The Golgi-apparatus is the site of synthesis of the cell wall matrix polysaccharides which includes the pectins and hemicelluloses. Following synthesis

by various glycosyltransferases, these polysaccharides are packaged in secretory vesicles on the *trans*-face of the Golgi-apparatus and transported to the cell wall. The third UDP-Glc pool is localized at the plasma membrane and is the product of plasma membrane associated sucrose synthase (pSuSy)[15].

Cellulose and callose are the only cell wall polymers synthesized at the plasma membrane[11]. Cellulose synthesis is catalyzed by multimeric enzyme complexes known as rosettes or terminal complexes located at the terminal ends of growing cellulose fibrils. UDP-Glc, the substrate for CeS, is provided at the site of synthesis by pSuSy which complexes with CeS[15,16]. The current model for pSuSy-mediated cellulose synthesis suggests that the effective synthesis of cellulose depends on the coordinated activity of both pSuSy and CeS. A consistent high correlation has also been shown between increased SPS activity and high rates of cellulose synthesis and secondary wall deposition[17]. Following synthesis of the glucan-polymer, multiple glucan polymers associate to form a crystalline microfibril.

CeS radial swelling (*rsw1*) mutants have disassembled CeS complexes, reduced cellulose synthesis capacity and its β-1,4-glucan accumulates in a noncrystalline form[18]. *Rsw1* mutants have a radial swelling phenotype similar to those of wild-type roots exposed to inhibitors of cellulose synthesis like dichlorobenzonitrile. CeS mutants also show defective elongation growth, collapsed xylem elements and resistance to the herbicide isoxaben, an inhibitor of cellulose synthesis during the formation of the primary cell wall[13]. A decrease in cellulose synthetic capacity is often partly compensated for by increases in cell wall pectin and hemicellulose[19].

1.4.2 SUCROSE SYNTHESIS

Apart from being the most important precursor for the hexose and pentose component of plant cell walls, UDP-Glc also provides Glc units for the synthesis of the main carbon transport and storage compound in plants, namely sucrose. The synthesis of sucrose in plants can occur by two separate enzymatic reactions:

$$\text{UDP-Glc + Fruc 6-P} \xleftrightarrow{SPS} \text{Suc 6'-P + UDP} \qquad (1)$$

$$\text{UDP-Glc + Fruc} \xleftrightarrow{SuSy} \text{Suc + UDP} \qquad (2)$$

Sucrose is synthesized in the chloroplasts of photosynthetic and in storage cells from UDP-Glc and fructose-6-P (Fru-6-P) in two sequential reactions catalyzed by SPS and sucrose-phosphate phosphatase (SPP, EC 3.1.3.24) (reaction 1)[20,21] as well as from UDP-Glc and fructose (Fru) by SuSy (reaction 2). SPS and SuSy are known to be cytosolic enzymes. Both reactions are reversible but it is generally accepted that the SPS reaction is irreversible

because of the rapid removal of the 6'-phosphate from sucrose-6-phosphate by SPP[8,22]. SPS is the main sucrose biosynthetic enzyme in source leaves and is also active in the futile cycle of simultaneous breakdown (by SuSy and cytosolic (neutral) invertase) and synthesis (by SuSy and SPS) which occurs in a variety of tissues[23]. Increased SPS activity, high levels of UDP-Glc and increased Glc-6-P are indicative of the onset of sucrose accumulation in sugarcane[22]. A rapid turnover of sugars in different compartments is characteristic of sucrose accumulation in storage and other non-photosynthetic cells and could be regulated by phosphorylated metabolites. The rapid cycling is referred to as a futile cycle because of the waste of energy associated with the simultaneous synthesis and breakdown of sucrose. The ongoing cycling of sucrose and hexoses allows the plant to rapidly respond to changes in the supply and demand for sucrose and to remove photoassimilates from source tissue to prevent sink inhibition of source activity.

The main sucrose synthetic activity in young photosynthetic tissue of sugarcane can be attributed to SPS[8], although the relative contribution of SPS and SuSy differs between plants and tissue type. Labeling experiments have indicated that in sugarcane, SPS is the major enzyme responsible for sucrose synthesis in mature tissue[8]. It is currently believed that SuSy is not as important in sucrose synthesis, but is more intimately concerned with the generation of UDP-Glc for cell wall synthesis. SuSy activity is associated with elongating young internodes and mature fully-elongated internodes and is suggested to be associated with sink strength based on tissue UDP-Glc demand[22]. SPS supplies a steady increase in sucrose content. In sugarcane the activity of SPS exceeds that of SuSy more than three-fold in mature tissue[8], and SPS was shown to be fully responsible for sucrose synthesis by internode 9.

1.4.3 SYNTHESIS OF CELL WALL MATRIX POLYSACCHARIDES

UDP-GlcA is the common precursor for activated glucuronosyl units and sugar nucleotides including UDP-GalA, UDP-Xylose (UDP-Xyl), UDP-Arabinose (UDP-Ara) and UDP-Apiose (UDP-Api), supplying the majority of monosaccharide units for hemicellulose and pectin biosynthesis. Three biosynthetic routes exist for the formation of UDP-GlcA in plants[4,24]. (1) UDP-galacturonate 4-epimerase (UGE, EC 5.1.3.6) can convert UDP-GalA to UDP-GlcA by a reversible C-4 epimerization reaction[4]; (2) GlcA-1-phosphate (GlcA-1-P), derived from the *myo*-inositol oxygenation pathway, is converted to UDP-GlcA by glucuronate-1-phosphate uridylyltransferase (EC 2.7.7.44)[4] and (3) UDP-Glc is converted to UDP-GlcA by UGD (UDP-α-D-glucose:NAD^+ 6-oxidoreductase, EC 1.1.1.22)[25].

1.4.3.1 UDP-GALACTURONATE 4-EPIMERASE

UGE, also known as galactowaldenase, catalyzes the reversible interconversion of UDP-Glc and UDP-Gal through epimerization of the C-4 OH-group. It is known to exist in plants, yeast, bacteria and animals[4,26]. UGE is part of the Leloir pathway of galactose metabolism. Epimerases are also known to exist for UDP-Xyl, UDP-GlcA and GDP-Man interconversion, catalyzing the following reactions[4,10]:

$$\text{UDP-Glc} \xleftrightarrow{UDP-Glc-4-epimerase} \text{UDP-Gal}$$

$$\text{UDP-Xyl} \xleftrightarrow{UDP-Xyl-4-epimerase} \text{UDP-L-Ara}$$

$$\text{UDP-GlcA} \xleftrightarrow{UDP-GlcA-4-epimerase} \text{UDP-GalA}$$

$$\text{GDP-Man} \xleftrightarrow{GDP-Man-3,5-epimerase} \text{GDP-L-Gal}$$

$$\text{GDP-Man} \xleftrightarrow{GDP-4-keto-6-deoxy-D-Man-3.5-epimerase-4-reductase} \xleftrightarrow{GDP-Man-4,6-dehydratase} \text{GDP-L-Fuc}$$

1.4.3.2 *MYO*-INOSITOL OXYGENATION PATHWAY

The metabolic pathways leading from *myo*-inositol to L-gulonic acid (precursor to L-ascorbic acid) and to GlcA was first described by Charalampous and Lyras (1957)[27]. Their work with ^{3}H and ^{14}C labeled *myo*-inositol indicated that label was incorporated into the galacturonosyl residues of pectin by strawberry fruit and parsley leaves. Incorporation of label into GlcA, Xyl, Ara and L-gulonic acid was also shown. The pathway responsible for the conversion of *myo*-inositol into UDP-GlcA is known as the *myo*-inositol oxygenation pathway (MIOP). The MIOP is often seen as a 'salvage' pathway for the synthesis of UDP-GlcA. Salvage pathways are alternative routes for the synthesis of nucleotide sugars in which free monosaccharides released by the degradation of polysaccharides and other glycoconjugates are phosphorylated by monosaccharide kinases and subsequently converted to nucleotide sugars by the action of pyrophosphorylases in the presence of nucleotide triphosphates as co-substrates[26,28,29]. Recent work indicated that *myo*-inositol oxygenase (MIOX, EC 1.13.99.1), the first enzyme of the MIOP, and UGD has different temporal and spatial expression patterns in *Arabibopsis*[3,30]. Both pathways are active in plant tissues and contribute UDP-GlcA for matrix polysaccharide synthesis in different ratios depending on the tissue type and developmental stage. It is important to note that where UGD is strongly inhibited by low levels of UDP-Xyl, none of the enzymes of the MIOP are[31]. This is an indication that under conditions where the synthesis of UDP-GlcA through UGD is inhibited by its downstream products, the MIOP will be able to supply the intermediates needed for cell wall synthesis.

Myo-inositol-1-P is synthesized from Glc-6-P by the action of 1L-*myo*-inositol-1-P synthase (EC 5.5.1.4)[32]. Free *myo*-inositol is generated by *myo*-inositol-1-P phosphatase (EC

3.1.3.25). The MIOP consists of three sequential reactions; (1) *myo*-inositol is converted to GlcA by MIOX, (2) GlcA is phosphorylated by glucuronokinase (EC 2.7.1.43), yielding GlcA-1-P and (3), UDP-GlcA is formed by the transfer of the uridylyl moiety of UTP by glucuronate-1-phosphate uridylyltransferase (EC 2.7.7.44). The reactions of the MIOP provide the precursor UDP-GlcA which is subsequently interconverted to GlcA, 4-O-methyl-GlcA, GalA, Xyl, Ara and Api and incorporated into glucuronoarabinoxylans (GAX) and related wall polymers.

1.4.3.3 UDP-GLUCOSE DEHYDROGENASE

UGD is a cytosolic enzyme which provides the precursor UDP-GlcA for the synthesis of UDP-Ara, UDP-Xyl, UDP-GalA, UDP-Api and their methylated derivatives[3]. GAX, synthesized from UDP-GlcA, UDP-Ara and UDP-Xyl contributes a substantial proportion of the cell wall in monocots[28] and as the above mentioned nucleotide sugars are all 'down stream' products of UGD, the biosynthesis of UDP-GlcA can be seen as a major metabolic activity during cell growth[33].

To fully understand the biosynthesis of polysaccharides it is necessary to investigate the upstream sources of the component nucleotide sugars[34]. The flux of carbohydrates into the pool of nucleotide sugars *via* UDP-GlcA is strictly controlled because it is generally accepted that UDP-GlcA cannot be reconverted into carbohydrates used to synthesize storage compounds like sucrose and the pools for storage compounds and nucleotide sugars used for wall synthesis are separated[30]. Interestingly, evidence suggests a link between UDP-GlcA metabolism and gluconeogenesis *via* UDP-Xyl as follows: *Myo*-inositol → GlcA → GlcA-1-P → UDP-GlcA → UDP-Xyl → Xyl → Xylulose → Xylulose 5-P → Pentose phosphate intermediates → Hexose phosphates[35]. In germinating seed or young growing tissues such a pathway would probably function to channel phytate derived from *myo*-inositol into substrates used for cell wall biosynthesis and to supply carbon based intermediates for energy production.

UGD was first described in and purified from bovine liver by Strominger and co-workers (1954)[36]. UDP-GlcA is formed by the NAD^+ dependent oxidation of UDP-Glc followed by the nucleophilic attack of a cysteine residue (Cys_{260}) in the catalytic domain on the resulting C6 aldehyde. The aldehyde intermediate is protected and tightly bound to the enzyme active site and is not accessible to external aldehyde-trapping reagents. The hydride is subsequently transferred to a second NAD^+ to form a thioester intermediate which is then hydrolyzed to form UDP-GlcA accounting for the irreversibility for the overall reaction[37,38]. Two NADH are formed. The enzyme mechanism is described as being of the Bi-Uni-Uni-Bi ping-pong type,

where UDP-Glc is bound first and UDP-GlcA is released last with NADH being released after each addition of NAD^+. UGD is a nucleotide sugar modifying enzyme that has both alcohol dehydrogenase and aldehyde dehydrogenase activity[37].

Extensive studies on the kinetics of UGD in animals and microorganisms[34,39] have been conducted. UGD from plant origin have received little attention possibly because of the early notion that an apparent predominance of the MIOP over UGD catalyzed formation of UDP-GlcA exist in some plants[24,40]. Although there is evidence for the existence of both pathways in plants, the relative contribution of these pathways to the synthesis of UDP-GlcA is unknown[33]. The expression pattern of UGD was analyzed in *Ugd* promoter::GUS and GFP transformed *Arabidopsis* plants[3]. Plants up to five days old showed strong expression in young roots but not in hypocotyls or cotyledons, while UGD was more evenly expressed in the vascular system of older plants, in flowers (stamen, stigma and nectaries) and in meristems of the leaf axil of rosette and inflorescence leaves. Tissues showing low or no UGD activity could efficiently incorporate ^{3}H-inositol into their cell walls indicating dominance of the MIOP. The expression of UGD in sugarcane was investigated in this laboratory (Institute of Plant Biotechnology, University of Stellenbosch, South Africa; IPB)[41]. The highest level of expression was detected in the leaf roll and internode 3 with a rapid decline in transcript levels down the stem and in older leaves. Almost no transcript could be detected in internode 18. Root tissue had a relatively high level of expression. Protein levels followed a similar pattern as transcript expression with almost no protein detected below internode 13.

UGD has been cloned from poplar (*Populus tremula x tremuloides*)[42] and soybean (*Glycine max*)[43,44]. Deduced amino acid sequences are highly similar between soybean, poplar, *Arabidopsis* and tobacco[33]. Native soybean UGD occurs as a homohexamer and has a molecular mass of approximately 272 kDa and a subunit mass of 50 to 52 kDa[43,45]. In contrast, the monomeric form of recombinant UGD from soybean was found to be the principal active from[44]. The enzyme was competitively inhibited by UDP-GlcA, UDP-Xyl and NADH[46]. An inducible UGD was purified from elicitor treated suspension culture cells of French bean (*Phaseolus vulgaris*) with a subunit mass of 40 kDa which showed alcohol dehydrogenase activity (K_m 1.8 ± 0.5 mM)[47]. Immunolocalization in hypocotyls showed that the enzyme was primarily expressed in the cytoplasm during the early stages of vascular differentiation when secondary walls are laid down. Work conducted in this lab (IPB) on UGD purified from sugarcane indicated that it had a MW of 52 KDa, was competitively inhibited by UDP-GlcA and UDP-Xyl, and in contrast to soybean UGD, was non-competitively inhibited by NADH[48]. Recently, Kärkönen and co-workers investigated the importance of the nucleotide sugar oxidation pathway in UDP-GlcA biosynthesis in developing maize (*Zea*

mays) organs[33]. Maize mutants were obtained by inserting transposons into either of two putative *Ugd* genes (*UDPGDH-A* and *-B*). Results indicated that both isozymes are active in young maize leaves and that the genes are developmentally regulated and transiently expressed in cells needing the precursors for wall biosynthesis. The disruption of UGD-A (specifically *udpgdh-A1* homozygotes) activity caused a reduction in cell wall pentose content, indicating that isozyme A is essential for UDP-GlcA synthesis, and that the remaining UGD activity (UGD-B) was not enough to supply adequate UDP-GlcA and UDP-pentoses. This also indicates that in young leaves of maize, the MIOP is not active enough to completely compensate for reduced UGD activity. Three UGD isozymes having high, intermediate and low K_m-values were subsequently detected in maize suspension-cultured cells[49]. Of note is that it was also shown that neither of the UGD isozymes had ADH activity in contrast to the findings of Robertson *et al.* (1996). Samac *et al.* (2004) expressed soybean UGD in transgenic alfalfa (*Medicago sativa*) plants under control of the phosphoenolpyruvate carboxylase (P4; enhanced xylem expression) and *Arabidopsis* class III chitinase (Atchit; enhanced phloem expression) promoters to target transgene over-expression to vascular tissue[50]. P4::UGD alfalfa plants had the highest UGD activity. Ten greenhouse grown lines had 200% more UGD enzyme activity than untransformed control plants. The enhanced activity was however not retained in mature field-grown transgenic lines in subsequent generations. The increase in UGD activity led to a decreased polysaccharide content in transgenic plants and increases in Xyl (15%) and Rha (36%) and a tendency toward increased Ara in cell walls. The relative increase in Xyl was much greater than the increase in Rha. The increase in Xyl and Ara can be explained by the increase in UDP-GlcA caused by the over-expression of UGD, but it is unclear why Rha was increased.

1.5 AIM OF THIS STUDY

In their review highlighting the main target areas of sugarcane sucrose metabolism for molecular targets to increase sucrose content, Grof and Campbell (2001)[1] suggest that for successful manipulation, it is necessary to identify the main rate limiting or co-limiting steps in all of the metabolic processes of sucrose biosynthesis and degradation. Thus, one of the important areas to consider is the futile carbon cycling between sucrose and hexose, resulting from the simultaneous synthesis (SuSy, SPS) and degradation (soluble acid invertase, cell wall bound acid invertase, neutral invertase, SuSy) of sucrose[22]. A by-product of sucrose breakdown, UDP-Glc, is also the precursor for the synthesis of structural polysaccharides, a respiratory substrate and a substrate for the re-synthesis of sucrose. As sugarcane is cultivated for its sugar-rich stalks, most carbon partitioning research in this plant has focussed on the accumulation of sucrose and its partitioning within the sugar pool. Relatively little attention has been paid to the allocation of carbon to the structural component of the cell[41]. The cell wall is known to be one of the largest carbon sinks in plants. For this reason its biosynthesis was chosen as site for genetic manipulation in an attempt to redirect carbon towards sucrose synthesis.

In the present study we investigate the effects of manipulation of the plant cell wall and in particular the UDP-Glc pool in sugarcane through the down-regulation of UDP-Glc dehydrogenase activity using antisense and RNAi based technologies. We hypothesize that a decrease in carbon flux through UGD would increase the UDP-Glc pool, thereby increasing the substrate for sucrose synthesis and accumulation of sucrose.

2. MATERIALS

All chemicals were obtained from **Sigma-Aldrich** (South Africa) unless otherwise indicated.
All nucleic acid modifying enzymes were from **Promega** (South Africa) unless otherwise indicated.
Primers were purchased from **Integrated DNA Technologies** (IDT, Whitehead Scientific, South Africa).
All coupling enzymes were obtained from **Roche** (South Africa) unless otherwise indicated.

3. METHODS

3.1 VECTORS, TRANSFORMATION AND MOLECULAR CHARACTERIZATION

3.1.1 Construction of silencing vectors

Antisense UDP-Glucose dehydrogenase vector

A full length *UGD* cDNA was isolated and characterized from a sugarcane cDNA library[41]. The antisense vector was constructed by cloning a 1760 bp *UGD* cDNA sequence in the antisense orientation into pUBI510 behind the cauliflower mosaic virus 35S and maize ubiquitin promoters to ensure constitutive expression. The *UGD* sequence was amplified from a full length UGD cDNA cloned into pBlueScript® SK(+) (Stratagene) by polymerase chain reaction[51] (PCR) using the primer pair UGD Fw 4: GCT CGA TAT CTG GTC ACA GAT CTA TCT G; Rev 5: TTA AGC GAC CGC GGG CAT GTC CTT GAG (1760 bp). Amplification conditions were as follows: 94 °C for 2 min; 35x (94 °C for 30 s, 58 °C for 30 s, 72 °C for 1.50 min); 72 °C for 5 min. EcoRI restriction sites on the primers was used to clone the insert into the corresponding pUBI510 restriction sites using T4 DNA ligase (Promega) according to standard procedures. Colony PCR using 35S F: TCC ACT GAC GTA AGG GAT GAC; UGD Fw 4: was used to select colonies with inserts in the antisense orientation.

Intron-spliced hairpin RNA vector

The ihpRNA vector used in this project was based on the high-throughput gene silencing vector pHANNIBAL[52]. The pHANNIBAL vector was obtained from Commonwealth Scientific and Industrial Research Organization Plant Industry (CSIRO, Canberra, Australia). The pHan-UGD vector was constructed from a 384 bp PCR product amplified from a full length sugarcane UGD cDNA cloned into pGEM®-T Easy (Promega). The PCR product was amplified from the 5' coding region and was cloned in both the sense and antisense

orientation into the pHANNIBAL directional cloning sites using restriction sites incorporated into the primers. Primers used for amplification and directional cloning were Xba.Xho UGD Fw: AGT CTC TAG ACT CGA GGG TTC GGT GGC TCT; Kpn.Hind UGD Rev: AGT CGG TAC CAA GCT TGG GGT CTC CCT GGT G. Amplification conditions were as follows: 94 °C for 2 min; 35x (94 °C for 30 s, 55 °C for 30 s, 72 °C for 30 s); 72 °C for 5 min. Standard molecular techniques were used for all steps in the construction of the vector[53]. Directional PCR using OCS Rev: CAC AAC AGA ATT GAA AGC AA; Kpn.Hind UGD Rev for the antisense insert, and 35S F; Kpn.Hind UGD Rev for the sense insert was used to identify positively transformed colonies. Amplification conditions for OCS Rev; Kpn.Hind UGD Rev and 35S F; Kpn.Hind UGD Rev were as follows: 94 °C for 2 min; 35x (94 °C for 30 s, 50 °C for 30 s, 72 °C for 30 s); 72 °C for 5 min. Both pAUGdf510 and pHan-UGD were transformed into, maintained and amplified in *E. coli* strain DH5α (Gibco-BRL).

3.1.2 Sugarcane transformation

Initiation and maintenance of sugarcane callus

Callus initiation, transformation and selection were carried out according to standard IPB procedures[54,55]. In brief, freshly harvested sugarcane (variety NCo310) stalks from a field (Welgevallen, Stellenbosch, South Africa) were surface sterilized using 96% EtOH. Outer leaves were removed to expose the leaf roll which was surface sterilized with 96% EtOH and flamed off. Working aseptically in a laminar flow cabinet, the outer leaf roll leaves were removed exposing the inner leaf roll which was cut into 0.5 cm sections and transferred to sterile MSC_3-media (MS-media containing 4.43 g/L MS basal medium, 2.22 g/L Gelrite Gellan Gum, sucrose 20 g/L, 0.5 g/L Casein enzymatic hydrolysate, pH 6.8 and 3 mg/L 2,4-Dichlorophenoxyacetic acid (2,4-D))[56]. Calli were grown at 28 °C in the dark and subcultured on fresh MSC_3-media every 14 days.

Microprojectile bombardment of embryogenic callus

After eight to ten weeks, actively growing embryogenic calli were selected for transformation and subcultured on fresh MSC_3-media 4 days prior to bombardment. The embryogenic calli were placed on MSC_3Osm (MSC_3 containing 0.2 M Sorbitol and 0.2 Mannitol (Merck)) medium for 4 hours prior to bombardment. EtOH (96%) sterilized 0.7 µm diameter tungsten Grade M17 (Bio-Rad) was used for bombardment. The final mixture of tungsten-plasmid preparation for bombardment contained 38.5 µg/µl tungsten, 0.08 µg/µl plasmid DNA, 963 mM $CaCl_2$ and 15 mM N-[3-aminopropyl]-1,4-butanediamine (Spermidine). Either pAUGdf510 or pHan-UGD together with pEmuKN, a selection plasmid that contains the neomycinphosphotransferase (*nptII*) gene driven by the maize Ubi-1 promoter, was used for transformation. The tungsten-plasmid preparation was fired into the calli in a 'gene gun'

under vacuum using 1200 kPa helium for propulsion. Approximately 4 hours after bombardment, the calli were transferred from MSC_3Osm to MSC_3.

Geneticin selection and regeneration

Two days after bombardment the calli were transferred to MSC_3G_{50} (MSC_3 containing 50 mg/ml Geneticin (Roche)) selection medium. Approximately eight to 12 weeks following bombardment, transformed calli were transferred to regeneration media (MSC) and incubated at 28 °C in the light. When plantlets were 3-6 cm high, they were transferred to autoclaved potting soil and hardened off.

3.1.3 Selection of transformants

Identification of transformants by polymerase chain reaction (PCR)

DNA was extracted from 10-20 mg tissue from either callus or leaves of young putative transgenic lines as described[57]. Young leaf tissue (10-20 mg) was frozen in liquid N_2 and ground in an Eppendorff tube. Four hundred µL extraction buffer (50 mM Tris-HCl, pH 8.0, 1% cetyltrimethylammonium bromide (CTAB)(Merck), 0.7 M NaCl, 10 mM EDTA, 0.5% polyvinylpirrolidone, 0.1% β-mercaptoethanol (BME, added just before use)) was added to the leaf tissue and vortexed for 10 sec. Tubes were then incubated for 60 min at 60 °C. Four hundred µL chloroform was added and samples were vortexed and centrifuged (16 000 xg, 5 min). The aqueous layer was transferred to new Eppendorff tubes containing 1 volume cold 100% isopropanol and incubated on ice for 15 min. The precipitated nucleic acid was centrifuged (16 000 xg, 10 min) and washed in 70% EtOH, dried and resuspended in 20 µL TE-buffer (10 mM Tris-HCl, pH 7.5, 1 mM EDTA) containing 20 µg/mL RNaseA. One µL of the DNA sample was used in PCR reactions to identify pAUGdf510; pEmuKN and pHan-UGD; pEmuKN co-transformed lines, respectively. Primer sets used were UGD Rev7: GCA CGG ATC CTT CAC CAT CTT GTC AGA TAC; CaMV-R: AGG GTT TCT TAT ATG CTC AAC (±400 bp) and 35S-F; Kpn.Hind-UGD Rev (370 bp) for pAUGdf510 and pHan-UGD respectively, and RNPTII-F: ACC ATG GTT GAA CAA GAT GGA TTG; RNTPII-R: CTC AGA AGA ACT CGT CAA GAA GG (799 bp) for pEmuKN. Amplification conditions for pAUGdf510 and pEmuKN were as follows: 94 °C for 5 min; 35x (94 °C for 30 s, 58 °C for 40 s, 72 °C for 30 s); 72 °C for 5 min. Amplification conditions for pHan-UGD were: 94 °C for 5 min; 35x (94 °C for 30 s, 50 °C for 30 s, 72 °C for 30 s); 72 °C for 5 min.

3.1.4 Plant material

Sugarcane plants (transgenic and wild type) were grown under greenhouse conditions (≈16 h light period, ≈25 °C). Wild type (WT) plants were regenerated from callus which was passed through tissue culture processes similar to those of the transgenic lines without

transformation. Three ripe stalks of each selected transgenic line were harvested. To limit metabolite losses, plant tissues (young leaf, YL; leaf roll, LR; internode 3+4 pooled, I3+4; internode 9+10 pooled (I9+10)) were cut into liquid N_2 directly after harvest and ground to a fine powder in an IKA® A11 basic (IKA) analytical mill. All tissues were stored in 50 mL screw cap tubes (Corning) at -80 °C.

3.1.5 DNA extraction and Southern blot analysis

Young leaves were collected from greenhouse grown mature sugarcane plants for screening of transgenic lines. Genomic DNA was extracted according to Dellaporta *et al.* (1983)[58]. Six grams of fresh plant material was cut into small pieces directly into liquid N_2 and ground in an IKA® A11 basic (IKA) analytical mill. The fine powder was transferred to a 50 mL sterile tube (Corning) containing 35 mL extraction buffer (100 mM Tris-HCl, pH 8.0, 0.5 M NaCl, 50 mM EDTA, 0.2% (v/v) BME) and shaken vigorously. 3.5 mL 20% (m/v) SDS was added and samples were incubated at 70°C for 60 min. Seven mL of 5 M potassium acetate was added and mixed and incubated on ice for 20 min. The cell debris was centrifuged (12 000 xg, 10 min, 4°C) and the supernatant added to 1 volume of ice-cold isopropanol and mixed. The precipitated nucleic acid was spooled off with a sterile Pasteur pipette hook and transferred to a 1.5 mL Eppendorff tube washed with 70% EtOH and dried. Nucleic acids were next resuspended in 1 mL 1 M NaCl containing 10 µg/mL RNaseA and incubated overnight at 37°C while rotating the tube. DNA was extracted with 1 volume chloroform: isoamyl alcohol (24:1, (v/v)) and precipitated with 1 volume of isopropanol (-20 °C, 60 min). DNA was resuspended and stored in 500 µL TE-buffer.

Ten µg DNA was digested overnight with 40 U HindIII/BamHI (Promega) and electrophoresed on 0.8% agarose gels, denatured and transferred to positively charged nylon membranes (Roche; Jhb, South Africa) by upward capillary transfer using 10 x SSC as buffer (20X SSC is 3 M NaCl, 0.3 M $Na_3C_6H_5O_7$, pH 6.8). Following transfer, DNA was crosslinked for 2.5 min at 120 mJ/cm using a UV-crosslinker (Ultra-Lūm Ultraviolet Crosslinker, Scientific Associates). Membranes were prehybridized for 2 h and hybridized for 4 h at 50 °C in RapidHyb™ (AEC-Amersham) in a revolving hybridization oven (Hybridization Oven/Shaker, AEC-Amersham). Single stranded α-^{32}P-dCTP (AEC-Amersham) labelled DNA probes were generated by asymmetric PCR[59] and size fractionated on Sephadex G-50 spin columns. UGD Fw4 was used to amplify the sense strand of the amplification product of UGD Fw4 and Rev5 (1760 bp). Amplification conditions were: 94 °C for 2 min; 40x (94 °C for 30 s, 58 °C for 30 s, 72 °C for 30 s); 72 °C for 5 min. Probes were denatured before being added to the hybridization buffer. Following hybridization, blots were rinsed once in 2 x SSC, 0.1% SDS for 20 min at room temperature, once in 2 x SSC, 0.1% SDS for 20 min at 50°C and once in 0.5 x SSC, 0.1% SDS for 20 min at 50°C and exposed to Super Resolution

Phosphor Screens for 12 h and visualized using a phosphor-imager and analysis software (Packard Cyclone, Packard Instrument Company Inc, USA).

3.1.6 RNA extraction and (Northern) blot analysis

Young leaf, leafroll, internode 3 and 4 as well as internode 9 and 10 tissue samples were collected from greenhouse grown mature plants for screening of transgenic lines. Total RNA was extracted from all tissues according to a modified method of Bugos *et al.* (1995)[60]. Tissues were cut into small pieces directly into liquid N_2 and ground in an IKA® A11 basic analytical mill. The fine powder was transferred to a 50 ml sterile tubes (Corning) in liquid N_2 and stored at -80 °C. Two grams frozen tissue was added to 10 mL homogenisation buffer (0.1 M Tris, pH 8.0, 1 mM EDTA, 0.1 M NaCl, 1% SDS (w/v), 0.1% BME) and 10 mL phenol:chloroform (1:1) in a 50 mL tube and vortexed. Sodium acetate, pH 5.2, was added to a final concentration of 0.1 M and the emulsion was incubated on ice for 15 min followed by centrifugation at 4 °C (12 000 xg, 15 min). The aqueous phase was transferred to a new tube containing 3 volumes 100% EtOH and 0.1 volume 3 M sodium acetate, pH 5.2, mixed and precipitated at -20 °C for two hours. The precipitated nucleic acid was centrifuged at 4 °C (12 000 xg, 15 min) and washed in 75% EtOH. Samples were resuspended in water and treated with Deoxyribonuclease I (RNase-free, Fermentas) according to the manufacturer's instructions followed by precipitation in 2.5 volumes 100% EtOH, 0.1 volume sodium acetate. Ten µg RNA was denatured in one volume formamide at 55 °C for 10 min before being loaded on 1.2% agarose gels. Following separation, the RNA was transferred to positively charged nylon membranes (Roche) by upward capillary transfer using 10 x SSC as buffer (20X SSC is 3 M NaCl, 0.3 M $Na_3C_6H_5O_7$, pH 6.8). RNA was crosslinked for 2.5 min at 120 mJ/cm using a UV-crosslinker. Membranes were prehybridized for 2 h and hybridized for 4 h at 65 °C in RapidHyb™. Single stranded α-^{32}P-dCTP labelled DNA probes were generated by asymmetric PCR as described (Southern Blots, above). UGD Rev3: CTC TTC TGG TAG TCG TTG ATC was used to amplify the non-sense strand of the amplification product of UGD Fw4; UGD Rev3. Amplification conditions were: 94 °C for 2 min; 40x (94 °C for 30 s, 54 °C for 30 s, 72 °C for 30 s); 72 °C for 5 min. Membranes were rinsed twice in 2 x SSC, 0.1% SDS at 25 °C and washed once for 20min in 1 x SSC, 0.1% SDS at 65 °C and exposed to Super Resolution Phosphor Screens for 12 h and visualized using a phosphor-imager and analysis software (Packard Cyclone, Packard Instrument Company Inc, USA).

3.1.7 Protein extraction and Western blot analysis

Western blots were performed according to Sambrook *et al.* (1989)[53]. Crude, desalted protein was denatured in 1 volume loading buffer (250 mM Tris, pH 6.8, 8 M urea, 40% glycerol) and 1 volume LB 2 (0.1 M DTT, 8% SDS, 0.01% Bromophenol Blue) at room

temperature before separation on SDS-PAGE using a 4% stacking gel and 12% separating gel. The Laemmli buffer system was used for all SDS-PAGE gels[61]. Gels were transferred to Hybond-C (AEC-Amersham) nitrocellulose membranes in transfer buffer (48 mM Tris, 39 mM glycine, 20% methanol and 0.0375% SDS) using a Trans-Blot SD semi-dry electrophoretic transfer cell (Bio-Rad).

Membranes were blocked in 1% BSA (Bovine Albumin (Fraction V), Roche) in TBST-buffer (20 mM Tris, pH 7.6, 137 mM NaCl, 0.1% Tween-20) for 2 h. The primary antibody (1:2000, polyclonal Rabbit anti- sugarcane UGD; UGD purified in this laboratory[48]) was added to the above buffer, incubated for 2 h and rinsed in TBST-buffer. The secondary antibody (1:7000, alkaline phosphatase conjugated mouse anti-Rabbit-IgG, Sigma) in TBST-buffer containing 3% low fat milk powder was then added and incubated for 1 h. The membrane was rinsed with TBST-buffer, washed twice in TBST-buffer containing 0.05% SDS and twice in TBST-buffer. Blots were developed using NBT/BCIP Ready-to-use tablets (Roche) as colour substrate.

3.2 METABOLIC CHARACTERIZATION

3.2.1 Assay for UDP-Glucose dehydrogenase activity

Crude protein extracts were made from YL, LR and young maturing internodal tissue (I3+4). The protein extraction buffer consisted of 50 mM Tris-HCl, pH 8.0, 2 mM EDTA and 5 mM dithiotreitol (DTT, Roche) which was added just prior to use. Extracts were centrifuged for 2 min (16 000 xg, 4 °C). Supernatants were transferred to new tubes and again centrifuged for 2 min (16 000 xg, 4 °C). Supernatants were transferred to Sephadex G-50 (Sigma-Aldrich) spin columns pre-equilibrated in extraction buffer and centrifuged for 2 min (2000 rpm, 4 °C). Desalted protein was added to assay buffer which consisted of 100 mM Tris HCl, pH 8.4 and 5 mM UDP-Glc (Roche) according to Kärkönen *et al.* 2005[49]. Reactions were started by adding NAD^+ (Roche) to a final concentration of 2 mM. The reduction of NAD^+ was monitored at 340 nm in a PowerWaveX spectrophotometer (Bio-Tek Instruments).

3.2.2 Sucrose and hexose extraction and enzymatic quantification

Frozen tissue (100 ± 10 mg) was added to 2 mL 80% EtOH, 100 mM potassium phosphate buffer pH 7. Suspensions were incubated at 70 °C for 1 h and centrifuged for 5 min (3500 xg, RT). Residues were re-extracted four times in 80% EtOH. Supernatants were pooled, vacuum dried overnight in a SpeedVac Plus SC11A (Savant), resuspended in 1 mL MilliQ H_2O (MilliPore) and either used directly for analysis or stored at -20 °C.

Enzymatic quantification was performed according to the method of Bergmeyer and Bernt[62]. For hexose analysis, 5 µL extract was added to 45 µL MilliQ H_2O and 200 µL buffer A (150

mM Tris pH 8.1, 5 mM $MgCl_2$, 1 mM ATP (Roche), 1 mM NADP (Roche)) in a 96 well microtitre plate (Nunc). Following an initial reading at A_{340}, 0.5 U of Hexokinase/Glucose 6-phosphate dehydrogenase (HK/G6-PDH) was added and incubated for 30 min at RT. A second reading was taken to calculate the free glucose content. Phosphoglucose isomerase (PGI, 0.7 U) was added and incubated for 30 min at RT. A third reading was taken to calculate the free fructose content present in the extract. To quantify the sucrose present in the sample, 5 µL of a 10x dilution of the extract was incubated with 40 µL buffer B (100 mM citrate pH 5.0, 5 mM $MgCl_2$) and 10 U β-Fructosidase (Roche) for 15 min at RT. Following the addition of 200 µL buffer A and 0.5 U HK/G6-PDH, samples were incubated and read as before. All spectrophotometric readings were performed using a PowerWaveX plate reader.

3.2.3 Assay for sucrose phosphate synthase activity

SPS activity was determined in source (YL) and sink (I9+10) tissues. SPS activity was assayed according to Baxter *et al*. (2003) under maximal (V_{max}) and limiting (V_{lim}) reaction conditions[63]. The protein extraction buffer consisted of 50 mM HEPES-KOH, pH 7.5, 10 mM $MgCl_2$, 1 mM EDTA, 10 mM DTT and Complete® (Roche) protease inhibitor cocktail tablets which was added just prior to use according to the manufacturers instructions. Extracts were centrifuged for 2 min (16 000 g, 4 °C). Supernatants were transferred to Sephadex G-25 (Sigma-Aldrich) spin columns pre-equilibrated in extraction buffer and centrifuged for 2 min (2000 rpm, 4 °C). Crude protein sample (100 µL) was incubated for 30 min at 35 °C with 100 µL assay buffer (50 mM HEPES-KOH, pH 7.5, 20 mM KCl and 4 mM $MgCl_2$) containing (a) V_{max} assay; 12 mM UDP-Glc, 10 mM Fruc 6-P and 40 mM Glc-6-P, or (b) V_{lim} assay; 4 mM UDP-Glc, 2 mM Fru-6-P, 8 mM Glc-6-P and 5 mM KH_2PO_4. The reaction was heated to 95 °C for 5 min to stop the reaction and was then centrifuged at 16 000 g for 5 min. 100 µL supernatant was added to 100 µL of 5 M KOH and incubated at 95 °C for 10 min to destroy unreacted hexose phosphates. After adding 200 µL anthrone reagent (0.14% anthrone in 14.6 M H_2SO_4) to 50 µL sample, absorbance was measured at 620 nm in a PowerWaveX spectrophotometer. The absolute amount of sucrose was calculated from a standard curve with 0-200 nmol sucrose.

3.2.4 Assay for sucrose synthase in the sucrose breakdown direction

To determine the rate of sucrose breakdown in source (YL) and sink (I9+10) tissues, the catalytic activity of SuSy was assayed according to Schäfer *et al* (2004)[84]. The protein extraction buffer consisted of 100 mM Tris-HCl, pH 7.0, 10 mM $MgCl_2$, 1 mM EDTA, 10 mM DTT and Complete® (Roche) protease inhibitor cocktail tablets which was added just prior to use according to the manufacturers instructions. Extracts were centrifuged for 2 min (16 000 g, 4 °C). Supernatants were transferred to Sephadex G-25 (Sigma-Aldrich) spin columns

pre-equilibrated in extraction buffer and centrifuged for 2 min (2000 rpm, 4 °C). Crude protein samples (20 µL) were incubated with assay buffer consisting of 100 mM Tris-HCl (pH 7.0), 2 mM $MgCl_2$, 400 mM sucrose, 2 mM NAD^+, 1 mM sodium pyrophosphate, 4 U/mL Phosphoglucomutase and 4 U/mL Glucose-6-phosphate dehydrogenase. Reactions were started by the addition of uridine diphosphate (UDP) to 2 mM. NADH production was monitored at 340 nm.

3.2.5 Assay for sucrose synthase in the sucrose synthesis direction

To determine the rate of sucrose synthesis in source (YL) and sink (I9+10) tissues, the synthetic activity of SuSy was assayed according to Schäfer *et al* (2004)[84]. The protein extraction buffer consisted of 100 mM Tris-HCl, pH 7.0, 10 mM $MgCl_2$, 1 mM EDTA, 10 mM DTT and Complete® (Roche) protease inhibitor cocktail tablets. Extracts were centrifuged and desalted as before (3.2.1, p22). Crude protein samples (20 µL) were incubated with assay buffer consisting of 100 mM Tris-HCl (pH 7.5), 15 mM $MgCl_2$, 20 mM UDP-glucose, 0.2 mM NADH, 1 mM phosphoenolpyruvate (PEP, Sigma-Aldrich) and 0.45 U/mL Pyruvate kinase/Lactate dehydrogenase (PK/LDH). Reactions were started by the addition of fructose to 10 mM. NAD^+ production was monitored at 340 nm.

3.2.6 Assay for UDP-glucose pyrophosphorylase activity

UDP-glucose pyrophosphorylase (UGPase) activity was determined in source (YL) and sink (I9+10) tissues. Crude protein was extracted and desalted as before (3.2.1, p22). Crude protein samples (20 µL) were incubated in assay buffer consisting of 100 mM Tris-HCl (pH 7.0), 2 mM $MgCl_2$, 10 mM UDP-glucose, 2 mM NAD^+, 4 U/mL Phosphoglucomutase, 4 U/mL Glucose-6-phosphate dehydrogenase. Reactions were started by the addition of sodium pyrophosphate to 1 mM. NADH production was monitored at 340 nm.

3.2.7 UDP-Glucose and hexose phosphate determination

Metabolite extractions were performed according to Stitt *et al*. (1989)[64]. Frozen tissue (500 ± 10 mg) was added to 800 µL ice cold 10% $HClO_4$, vortexed and incubated at 4 °C for 20 min with mixing. Insoluble material was centrifuged for 2 min (13 000 rpm, at 4 °C). Following removal of the supernatant, the pellet was washed and incubated for 15 min with 250 µL 2% $HClO_4$, centrifuged for 2 min (13 000 rpm, 4 °C), and pooled with the first supernatant. Samples were neutralized (pH 7.0-7.5) by the addition of 5 M KOH, 1 M triethanolamine and incubated at 4 °C for 15 min. The insoluble $KClO_4$ was centrifuged for 2 min (13 000 rpm, RT).

Supelclean 100 mg ENVI-Carb SPE (Supelco) columns was activated with 3 mL 80% acetonitrile, 0.1% trifluoroacetic acid (TFA) (Fluka), followed by 3 mL H_2O according to Räbina *et al.* (2001)[65]. The supernatants were applied to the columns and the flow-through containing the hexose phosphates collected. The columns were washed with 3 mL H_2O, 3 mL 25% acetonitrile and 3 mL 50 mM triethylammonium acetate (TEAA) buffer (Fluka) pH 7.0. The NDP-sugars were eluted with 3 mL 25% acetonitrile (Merck), 50 mM TEAA buffer, pH 7.0. All sugar-phosphate and nucleotide sugar samples were frozen in liquid N_2 and vacuum dried in a SpeedVac Plus SC11A.

Hexose phosphates were resuspended in 250 µL MilliQ H_2O. 50 µL sample was added to 175 µL reaction buffer containing 100 mM Tris, pH 8.0, 5 mM $MgCl_2$ and 0.25 mM NADP in a 96-well plate. The background was read at A_{340}. 0.7 U G6-PDH, 0.7 U PGI and 0.2 U phosphoglucomutase (PGM) in 5 mM Tris-HCl, pH 8.0 were added sequentially, incubated for 15 min at RT and read at A_{340} to determine Glc-6-P, Fru-6-P and Glc-1-P respectively.

Nucleotide sugar containing samples were resuspended in 250 µL MilliQ H_2O. 50 µL sample was added to 200 µL of reaction buffer containing 100 mM Tris, pH 8.0, 5 mM $MgCl_2$ and 0.25 mM NADP. Background readings were taken as before. 0.2 U UDP-glucose pyrophosphorylase (Sigma-Aldrich) and sodium pyrophosphate to a final concentration of 15 mM were added and samples were incubated for 20 min at RT and read as before.

3.2.8 Protein determination

Protein concentration was determined according to Bradford[66] using a commercially available protein assay solution (Bio-Rad). Bovine Albumin (Fraction V) (Roche) was used as protein standard.

3.3 CELL WALL ANALYSIS

3.3.1 Preparation of alcohol insoluble residue (AIR)

Frozen tissue (100 ± 10 mg) was added to 100% EtOH to give a final concentration of 80% (v/v) and incubated at 70 °C for 20 min. Samples were centrifuged (4000 xg) and supernatants were discarded. The extraction process was repeated four times using 80% EtOH. AIR samples were washed in acetone and vacuum dried in a SpeedVac Plus SC11A (Savant) and stored in air-tight screw top tubes in a desiccator under vacuum.

3.3.2 Hydrolysis of alcohol insoluble residue

Seaman hydrolysis

Destarched AIR (10 ± 1 mg) was weighed into a screw top tube and 200 µL 12 M H_2SO_4 was added and vortexed. Samples were incubated at 4 °C for 2 hr. Subsequently, the H_2SO_4 was diluted to 2 M and incubated at 80 °C for 2 hr to hydrolyze cell wall polysaccharides.

Trifluoroacetic acid hydrolysis

Destarched AIR (1 ± 0.1 mg) was weighed into screw-top tubes and 0.5 mL 2 M TFA (Fluka) added. The non-cellulosic polysaccharide was hydrolyzed[12] at 121 °C for 1 hr. Following hydrolysis, tubes were cooled to RT and the TFA resistant cellulosic residue was centrifuged (5000 rpm, 2 min). The supernatants were transferred to new tubes. The cellulosic residue was washed twice with 0.5 mL MilliQ H_2O. Supernatants were pooled and vacuum dried in a SpeedVac overnight to remove TFA. To remove residual TFA, hydrolyzed monosaccharides were dissolved in 1 mL methanol, and vacuum dried. This process was repeated three times. Hydrolyzed monosaccharides were stored under vacuum over self-indicating silica-gel.

3.3.3 Determination of cell wall total uronic acids

This is an adaptation of the methods of Blumenkrantz and Asboe-Hansen (1973) and van den Hoogen *et al.* (1998)[67,68]. Forty µL hydrolyzed AIR sample containing 0.5-8 µg uronic acid was added to a microtiter plate (Nunc) well. Two hundred µL 96% H_2SO_4 containing 120 mM sodium tetraborate (Fluka) was added. Samples were incubated for 30 min at RT and the background was read at A_{530}. 40 µL *m*-hydroxydiphenyl reagent (100 µL *m*-hydroxydiphenyl in DMSO (SAARChem), 100 mg/mL, mixed with 4.9 mL 80% (v/v) H_2SO_4; made freshly just before use), was added and mixed. Samples were then incubated at RT for 15 min and read in a PowerWaveX spectrophotometer (Bio-Tek Instruments) at 530 nm. Galacturonic acid (Fluka) was used as standard (0 to 8 µg).

3.3.4 Assay for *myo*-inositol oxygenase activity

MIOX activity was assayed according to Reddy *et al.* (1981)[69] with minor modifications. Crude protein was extracted in extraction buffer containing 100 mM Tris-HCl, pH 7.6, 2 mM L-cysteine, 1 mM ammonium ferrous sulfate hexahydrate (Fluka), 1 mM EDTA and 1% polyvinylpolypyrrolidone (PVPP). Following extraction, samples were centrifuged for 5 min (16 000 xg, 4 °C). Supernatants were transferred to new tubes and 1 volume 50% (v/v) polyethylene glycol 6000 (PEG) was added and samples were incubated on ice for 30 min and centrifuged for 10 min (10 000 xg, 4 °C). Supernatants were discarded and pellets resuspended in 100 mM potassium phosphate buffer, pH 7.2, containing 2 mM L-cysteine and 1 mM ammonium ferrous sulfate hexahydrate.

MIOX activity was assayed using 50 µg crude desalted protein in 100 mM potassium phosphate buffer, pH 7.2, containing 2 mM L-cysteine and 1 mM ferrous ammonium sulfate hexahydrate. Reactions were started by the addition of *myo*-inositol to a final concentration of 60 mM. Reactions were incubated for 30 min at 30 °C. Glucuronic acid formed was determined by the 3-phenylphenol method[68]. D-GlcA was used as standard.

3.3.5 Expression analysis of *UGD* and *MIOX*

Recently published sequences for *MIOX* from mouse, rat, human[70] and *Arabidopsis*[30] was used as a starting point to obtain a consensus sequence constructed from EST's from The Institute for Genomic Research *Saccharum officinarum* Gene Index (TIGR-SoGI, http://www.tigr.org/tigr-scripts/tgi/T_index.cgi?species=s_officinarum) and the National Center for Biotechnology Information (NCBI) databases using the Basic Local Alignment Search Tool (BLAST, http://www.ncbi.nlm.nih.gov/BLAST/) algorithm[71]. The TIGR-SoGI was also used to screen different tissue EST libraries for differential expression patterns of *UGD* for comparison with the expression of *MIOX* in the same libraries.

3.3.6 Semi-quantitative expression analysis of *UGD* and *MIOX* using RT-PCR

Five microgram total RNA extracted from young internodal tissue of sugarcane lines with reduced *UGD* activity was reverse transcribed using SuperScript III (Invitrogen) and used for semi-quantitative reverse transcription (RT)-PCR. *MIOX* cDNA transcripts were amplified using Miox1 Fw: GAT CCA TCG GGG AAG AAG AT; Miox1 Rev: GTT GAA CTT GGG GTT GTG GT (597 bp) designed from TC51845 obtained from TIGR-SoGI. *UGD* transcripts were amplified using UGD Fw4; UGD Rev3 (900 bp). *α-Actin* was used as a housekeeping control to allow for comparison of the amount of template. Primers used for *α-actin* were actin Fw1: TCA CAC TTT CTA CAA TGA GCT; actin Rev1: GAT ATC CAC ATC ACA CTT CAT (600 bp). Amplification conditions for *MIOX* and *actin* were as follows: 94 °C for 2 min; 35x (94 °C for 30 s, 55 °C for 30 s, 72 °C for 30 s); 72 °C for 5 min. Conditions for *UGD* was: 94 °C for 2 min; 30x (94 °C for 30 s, 58 °C for 40 s, 72 °C for 30 s); 72 °C for 5 min. Each primer pair amplified a single product. Products were separated on 1% agarose gels and stained with ethidium bromide. Digitized images were analysed using AlphaEaseFC™ Software Version 4.0.1 (Alpha Innotech Corporation).

3.3.7 Destarching of alcohol insoluble residue and assay for starch content

To remove starch, alcohol insoluble residues were resuspended in MilliQ water and incubated at 100 °C for 60 minutes. Samples were left to cool to room temperature and 4 U amyloglucosidase (AMG) from *Aspergillus niger* (Fluka) in 5 mM sodium acetate buffer, pH 4.8, was added. Samples were incubated overnight at 55 °C. Following incubation, samples

were centrifuged (4000 xg) and washed twice in 70% EtOH. All supernatants were pooled and vacuum dried and resuspended in MilliQ water for starch determination. AIR was washed twice in 100% acetone. Destarched AIR was dried under vacuum and stored in air-tight screw top tubes in a desiccator under vacuum. Background glucose and glucose released by AMG was determined according to the method of Bergmeyer and Bernt (1974)[62].

3.3.8 Enzymatic quantification of cell wall glucose content

To determine the non-cellulosic glucose content of young leaves, ten mg of dry AIR (starch removed by AMG, 3.3.7, p27-8) was incubated in 2 M TFA at 100 °C for 5 hr. The cellulosic residue was centrifuged, washed twice with 70% EtOH and dried. All supernatants were pooled, vacuum dried and resuspended in MilliQ water.

The remaining cellulosic residues were hydrolyzed by Seamann hydrolysis (3.3.2, p26), neutralized with NaOH, vacuum dried and resuspended in MilliQ water. The glucose content of cellulose was determined as before (3.2.2, p 22-3)[62].

3.3.9 Monosaccharide derivatisation and analysis by GC-MS

All TFA hydrolyzed samples and standards were derivatised according to the method of Roessner *et al.* (2000)[72]. Eighty µL methoxyamine HCl in pyridine (20 mg/mL) was added to dry samples, vortexed thoroughly and incubated at 30 °C for 90 min with intermittent vortexing. Next, 20 µL of an alkane mixture (n-dodecane, n-pentadecane, n-nonadecane, n-docosane, n-octacosane, n-dotriacontane and n-hexatriacontane) used for retention time standards followed by 140 µL N-Methyl-N-(Trimethylsilyl)-triflouroacetamide (MSTFA) was added and incubated at 37 °C for 30 min. Samples were kept at RT for two hours before injection.

Sample volumes of one µL were injected with a splitless injection. The flow rate was 1 mL min^{-1}. The system consisted of an AS 2000 autosampler, trace GC and a quadropole trace MS (ThermoFinnigan). Gas chromatography was performed on a 30 m Rtx®-5Sil MS column (RESTEK) with Integra Guard with an inner diameter of 0.25 mm and 0.25 mm film thickness. Injection temperature was 230 °C and the ion source temperature was set at 200 °C. The temperature program was as follows: 5 min at 70 °C, followed by a 1 °C min^{-1} oven ramp to 76 °C and a second ramp of 6 °C min^{-1} to 350 °C. The system was then temperature equilibrated at 70 °C before injection of the next sample. Mass spectra were recorded at two scans per sec with a scanning range of 50-600 *m/z*. Chromatograms and mass spectra were evaluated using the Xcalibur™ software bundle version 1.2 (Finnigan Corporation 1998-2000).

3.3.10 Statistical analysis

The Student's t-test (two-sample, independent-groups) was used to test for significant differences between group means. The square of the Pearson product moment correlation coefficient (coefficient of determination) was calculated to indicate correlation between characteristics. STATISTICA (StatSoft, Inc. (2004)(data analysis software system), version 7. www.statsoft.com) was used throughout for all statistical analysis. Statistical significance was defined as $P \leq 0.05$.

4. RESULTS

In the present study, antisense and RNAi based techniques were used to silence UDP-Glucose dehydrogenase and decrease its activity *in planta*. The aim was to manipulate the plant cell wall synthesis and in particular the UDP-Glc pool in sugarcane. We hypothesize that a decrease in carbon flux through UGD would increase the UDP-Glc 'pool', thereby increasing the substrate for sucrose synthesis and subsequently the accumulation of sucrose. In the following sections we discuss the results of transformation vector construction, sugarcane transformation and molecular-, metabolic- and cell wall characterization of transgenic plants with repressed UGD activity.

NOTE: for comparative purposes, all transgenic lines were numbered according to their percentage of wild-type UGD activity in leaf roll tissue. The following convention was used for naming purposes throughout the text: an **A** for **pAUGdf510** or an **H** for **pHan-UGD** followed by the % leaf roll UGD activity. Lines which were not included in further detailed analysis lack the A or H. Only antisense lines were characterized in detail due to limited amounts of tissue available in pHan-UGD transformed lines which were not fully mature at the time of tissue sampling.

4.1 VECTORS, TRANSFORMATION AND MOLECULAR CHARACTERIZATION

4.1.1 Transformation vector construction

In order to reduce the expression of *UGD*, a 1.65 kb *EcoRI* fragment was isolated from a full-length *UGD* cDNA and cloned in the reverse orientation downstream to the CaMV 35S and ubiquitin promoters into the *EcoRI* site of pUBI510. The resulting 'antisense' *UGD* plasmid (designated pAUGdf510, Figure 4.1 A, p.31) was verified by restriction analysis and directional PCR (data not shown) to confirm insert orientation. As an alternative approach to reduce *UGD* expression in sugarcane, a 384 bp fragment amplified from *UGD* cDNA was cloned in both sense (*XhoI/KpnI* fragment) and antisense (*HindIII/XbaI* fragment) orientation downstream to the CaMV 35S promoter and on either side of the Pdk-intron into pHANNIBAL. The resulting intron-spliced hairpin RNA vector (designated pHan-UGD, Figure 4.1 B, p.31) was verified as before (data not shown).

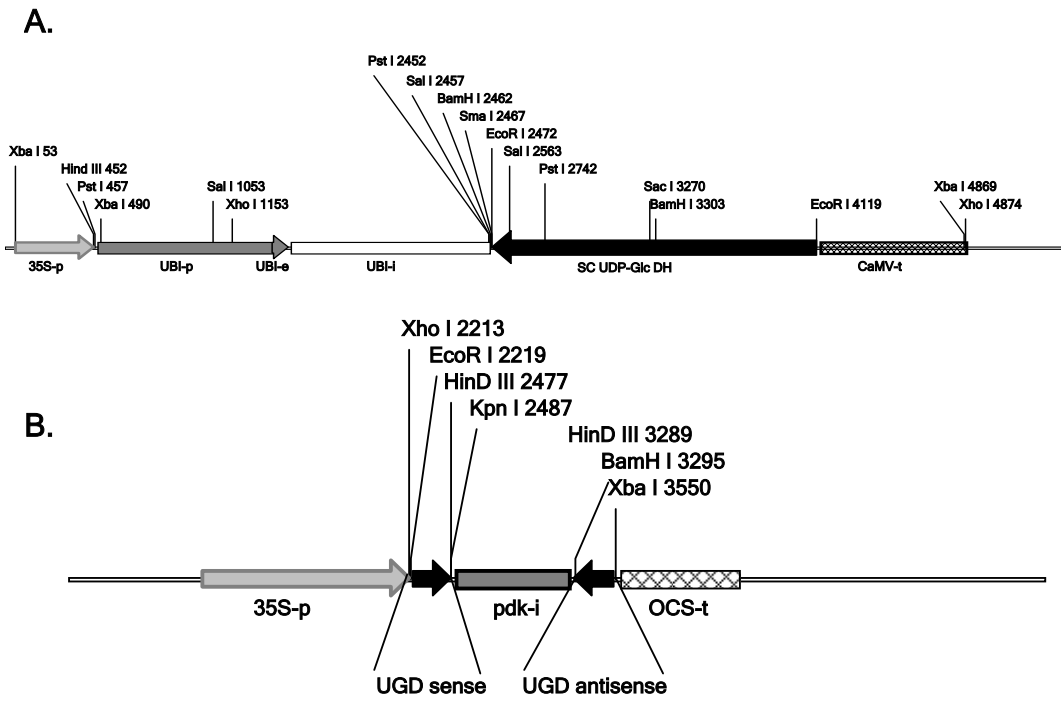

Figure 4.1: Schematic representation of a section of pAUGdf510 and pHan-UGD.

The pAUGdf510 vector (7051 bp) is based on pUBI 510 and contains a 1647 bp insert of the full length *UGD* gene in the antisense orientation. pAUGdf510 is constitutively expressed by the cauliflower mosaic virus (CaMV) 35S (35S-p) and maize ubiquitin (UBI-p) promoter and contains the CaMV termination sequence (CaMV-t). (**B**) The pHan-UGD vector (6342 bp) is based on pHANNIBAL and contains two 384 bp inserts of the *UGD* gene in both the sense and antisense orientation separated by the Pdk-intron (pdk-i). pHan-UGD is constitutively expressed by the CaMV 35S promoter and contains the octopine synthase termination sequence (OCS-t). Bacterial ampicillin resistance was used for selection.

4.1.2 Confirmation of putative transgenic lines

To select positively transformed clones, transformants were screened by means of PCR for the presence of both the silencing vector and pEmuKN. For each transformation 15 independent regenerated plants that were resistant to geneticin were transferred to soil and hardened off under standard conditions. Nine and four lines were generated which were transformed with the pAUGdf510 (Figure 4.2, p.32) and pHan-UGD (Figure 4.3, p.32) respectively.

Four antisense lines were selected for further analysis based on UGD protein levels as indicated by Western blot analysis (4.1.5, p.35). Line 1.4 (transformed with pHan-UGD) was not selected for analysis because of lack of growth of plants in this line. Only basic metabolic

and expression analysis was attempted in pHan-UGD transformed lines due to very little tissue being available for analysis.

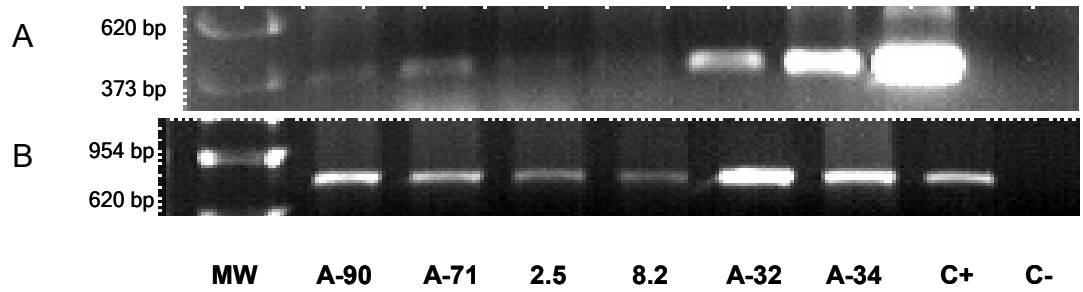

Figure 4.2: PCR amplification of the transgene in putative pAUGdf510 transformed sugarcane lines. DNA was extracted from young leaf tissue. 150 ng DNA was used for amplification. Primer pairs used were (**A**) 35S-F and UGD Rev7 for the pAUGdf510 plasmid, and (**B**) R-NPT II F and R-NPT II R for the co-transformed pEmuKN. MW, molecular weight marker, C+ positive control (pAUGdf510), C- negative control.

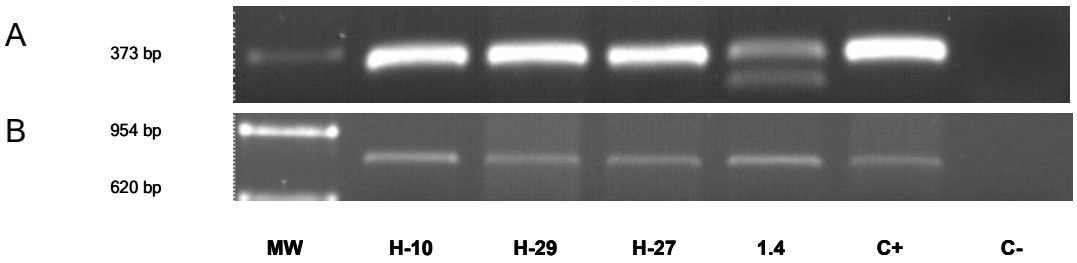

Figure 4.3: PCR amplification of the transgene in putative pHan-UGD transformed sugarcane lines. DNA was extracted from 10 mg calli. Primer pairs used were (**A**) 35S-F and Kpn.Hind-UGD Rev to detect pHan-UGD, and (**B**) R-NPT II F and R-NPT II R for the co-transformed pEmuKN. MW, molecular weight marker, C+ positive control (pHan-UGD), C- negative control.

4.1.3 DNA (Southern) blot analysis

To confirm that transgenic lines were products of different transformation events, Southern analysis was used to confirm the presence of the transgene (pAUGdf510) in putative transformed sugarcane lines (Figure 4.4, p.33). ^{32}P-labelled ssDNA probes were used to detect endogenous *UGD* genes as well as the transgene. Figure 4.4 shows distinct banding patterns in selected transgenic lines and confirms that the lines used in subsequent analyses are unique.

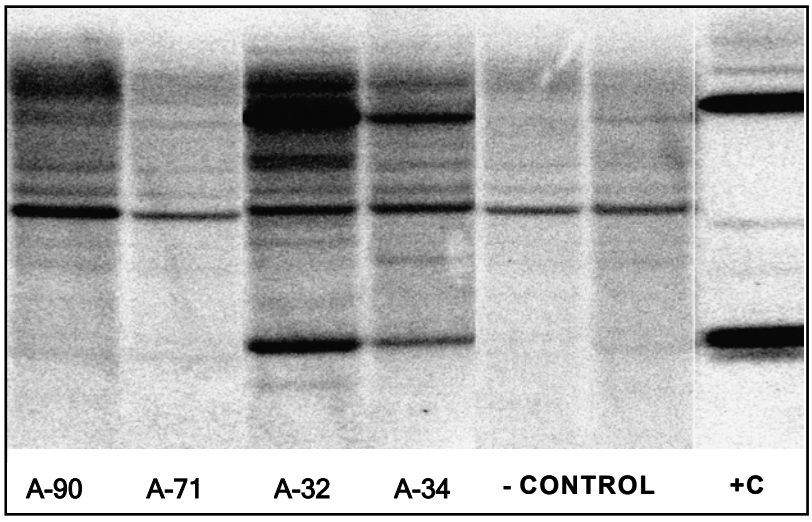

Figure 4.4: Southern analysis of transgenic sugarcane lines transformed with pAUGdf510. 10 µg DNA from leaves of selected transformed lines was digested with *BamHI/HindIII*, electrophoresed and transferred to a positively charged nylon membrane. The blot was probed with a labelled ssDNA UGD Fw4; UGD Rev5 probe.

4.1.4 Northern blot analysis

To select plants with reduced *UGD* transcript level, selected transformants were screened by Northern analysis. Amongst plants transformed with pAUGdf510 several lines were identified with reduced *UGD* mRNA of which four lines were selected for more detailed metabolic and structural characterization (Figure 4.5, p.34). The strongest transcription level inhibition was found in line A-34 although inhibition in all lines was similar.

Similarly, young leaves of selected transgenic lines transformed with pHan-UGD were screened for *UGD* transcript level by Northern analysis (Figure 4.6, p.34). All of the four lines that were successfully regenerated showed reduced *UGD* transcript levels. Line 1.4 had the lowest UGD mRNA levels but was not included in subsequent determinations because of lack of growth in this line.

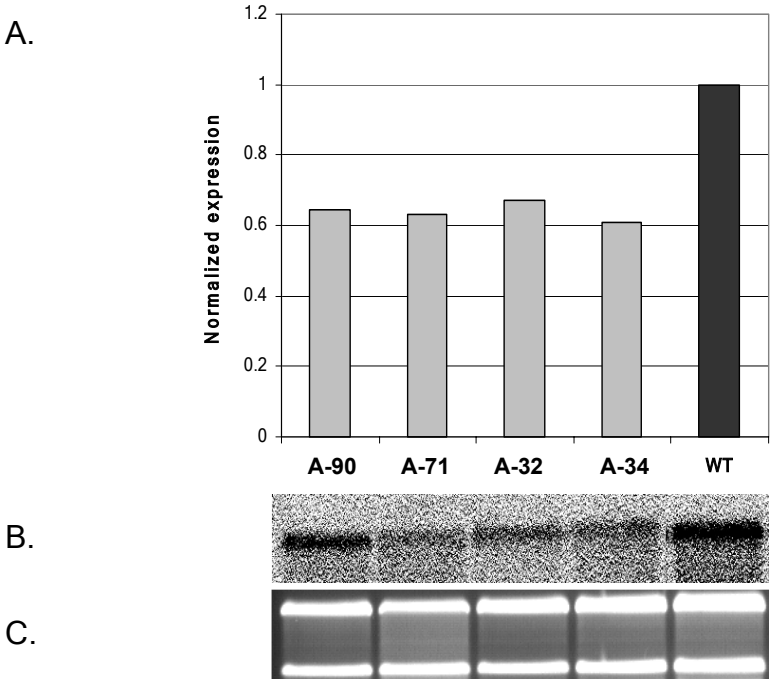

Figure 4.5: Northern analysis of transgenic sugarcane lines transformed with pAUGdf510. **A.** Normalized *UGD* transcript level in leaf roll. **B.** Northern analysis on 10 µg total RNA showing the repression of endogenous *UGD* transcription in selected confirmed transgenic lines and wild type (WT) sugarcane. **C.** RNA gel stained with ethidium bromide.

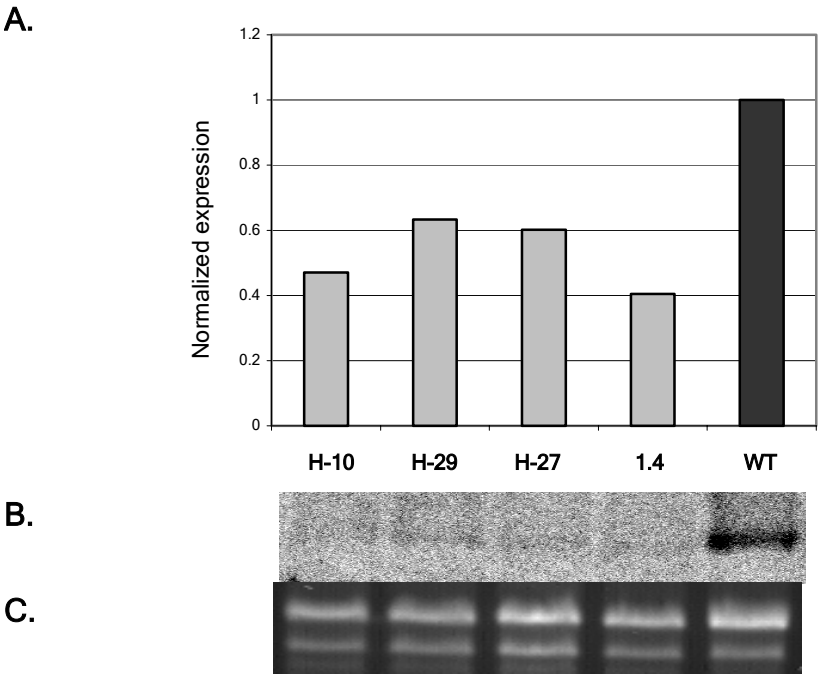

Figure 4.6: Northern analysis of transgenic sugarcane lines transformed with pHan-UGD. **A.** Normalized *UGD* transcript level in young leaf. **B.** Northern analysis on 10 µg total RNA showing the repression of endogenous *UGD* transcription in selected confirmed transgenic lines and wild type (WT) sugarcane. **C.** RNA gel stained with ethidium bromide.

4.1.5 Western analysis of UGD-Glucose dehydrogenase activity in sugarcane with repressed *UGD* expression

Western blots were used to investigate the effect of antisense repression of *UGD* expression on the level of UGD protein in the leaf roll of transgenic sugarcane. Western blot analysis was carried out using a polyclonal antiserum raised against UGD from sugarcane. In agreement with the reduction shown in the transcript levels of UGD in pAUGdf510 transgenic lines, UGD protein amount was reduced in selected lines as compared to control plants. Among the transgenic lines, A-34 had the lowest level of UGD protein, followed by A-32.

Figure 4.7: Western analysis of sugarcane transformed with pAUGdf510.

Leaf rolls of transgenic sugarcane were harvested and crude protein were extracted and desalted. Five µg crude protein was loaded per lane and electrophoresed on a 12% SDS-PAGE gel, transferred to nylon membranes and probed with a polyclonal rabbit anti-sugarcane UGD antibody.

4.2 METABOLIC CHARACTERIZATION

Although the effects of *UGD* mutants lacking UGD activity and of overexpression of UGD on cell wall synthesis have been studied in maize[33,49] and *Alfalfa*[50] respectively, the effect of repression of *UGD* expression on sucrose synthesis have not been considered. In the present investigation UGD activity was chosen for down regulation to determine the effect of a decrease in the flux of UDP-Glc toward the hemicellulose and pectic polymer component of the cell wall might have on the accumulation of sucrose in sugarcane. The effect of antisense repression on UGD activity and related metabolism is considered in the present chapter with substantiation of results by data from intron-spliced hairpin RNA repressed UGD activity in sugarcane.

4.2.1 UDP-Glucose dehydrogenase activity in sugarcane transformed with antisense and ihpRNA constructs

To investigate the role of UGD (Section 1.4.3.3, p.13-5) in sugarcane carbon metabolism, its expression was decreased by either antisense repression or by using an RNA interference approach. The antisense vector (pAUGdf510) contained a full length *UGD* cDNA in antisense orientation behind the cauliflower mosaic virus 35S (CaMV 35S) and maize ubiquitin promoters. The RNAi vector (pHan-UGD, based on pHANNIBAL, CSIRO)

contained a UGD fragment in antisense and sense orientation on either side of a spliceable intron sequence and was driven by the CaMV 35S promoter.

Desalted, crude protein extracts from plants showing antisense repressed *UGD* expression and wild-type control plants were assayed for UGD activity (Figure 4.8). UGD activity in line A-34 decreased by 83.5 ± 2.5% in internode 3+4 and 65.8 ± 13.1% in the leaf roll which represented the most significant silencing (P = 0.005 and P = 0.006 respectively) of UGD activity in antisense-lines. The UGD activity in leaf roll tissue of plants transformed with pAUGdf510 was also correlated with the UGD protein level as indicated by Western blot analysis (Section 4.1.5, p.34 and Figure 4.7, p.35).

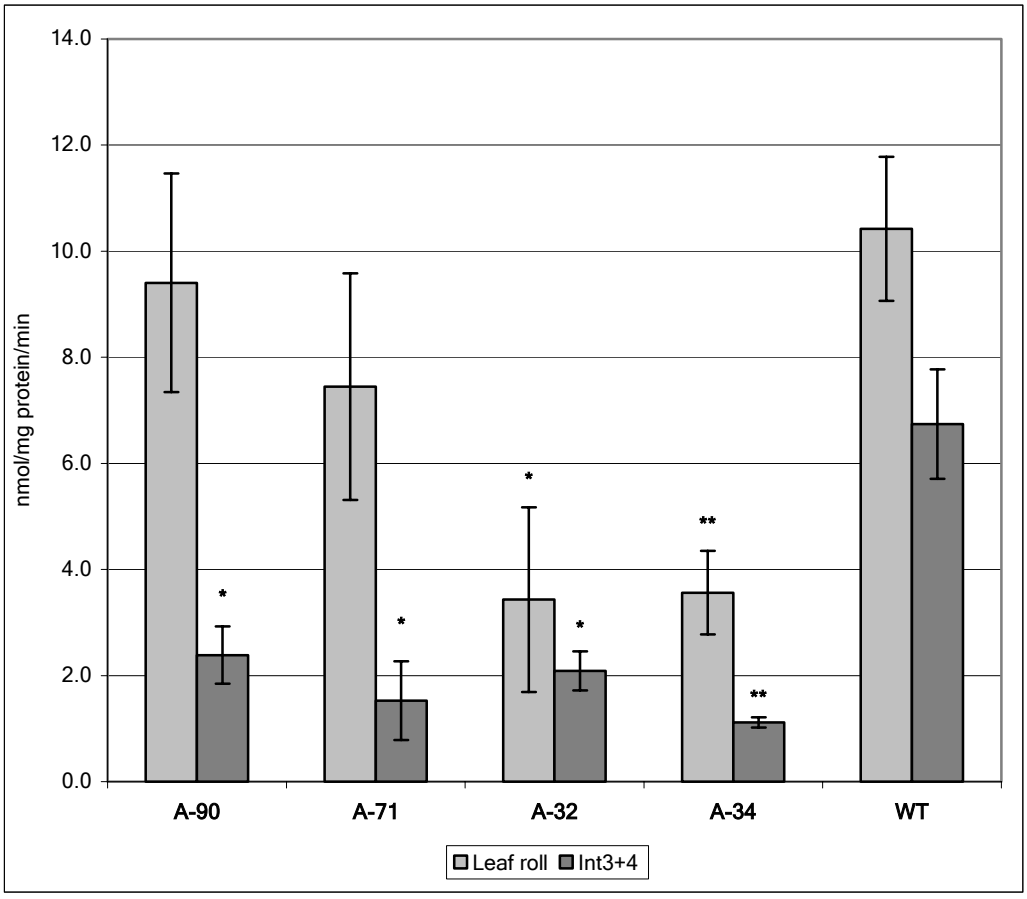

Figure 4.8: Repression of UDP-Glucose dehydrogenase activity in sugarcane transformed with pAUGdf510. Crude desalted protein extracts from the leaf roll and internode 3-4 (Int 3+4) were used to determine UGD activity. Values calculated as mean ± SEM. A-90 – A-34, n = 3; WT, n = 5. * $P \leq 0.05$; ** $P \leq 0.01$

Sugarcane lines transformed with pHan-UGD showed similar decreases in UGD activity (Figure 4.9, p.37) as was found in the antisense lines. Silencing of UGD activity in leaf roll

tissue was significant ($P \leq 0.05$) across all lines. Although silencing was evident in young internodal tissue (internode 3-5), only line H-27 showed a significant decrease ($P = 0.01$) in UGD activity.

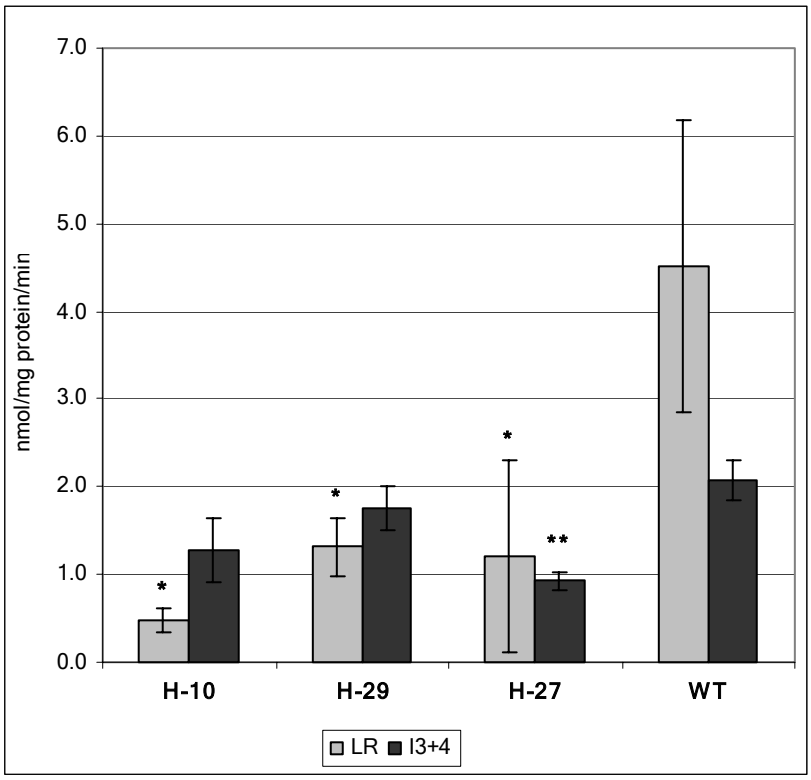

Figure 4.9: Repression of UDP-Glucose dehydrogenase activity in sugarcane transformed with pHan-UGD. Crude desalted protein extracts from the leaf roll and internode 3+4 (Int 3+4) were used to determine UGD activity. Values calculated as mean ± SEM. H-10 - WT, n = 3. * $P \leq 0.05$; ** $P \leq 0.01$

4.2.2 Sucrose and hexose accumulation in sugarcane with repressed *UGD* expression and enzyme activity

To analyze the effect of repressed *UGD* expression and decreased enzyme activity on the accumulation of sucrose, glucose and fructose in transgenic sugarcane, metabolites were extracted and determined using an enzymatic method (Figure 4.10, Table 4.1 and 4.2, p.38-9). Line A-34 showed a significant increase in sucrose storage in young (LR, $P = 0.02$), maturing (Int 3+4, $P = 0.01$) and mature internodes (Int 9+10, $P = 0.05$). Lines A-90 and A-71 also showed significantly increased sucrose accumulation in mature internodes. When calculated on average percentage sucrose (in LR, Int 3+4 and Int 9+10) per fresh weight basis, line A-34 had 17.9 ± 4.3% (n = 3) sucrose per gram fresh weight compared to 10.0 ± 2.3% (n = 6) of control plants.

The increased sucrose concentration was highly correlated with decreased UGD activity (Section 4.3.1, p35-7) in internode 3+4 of line A-32 and A-34 with line A-32 showing the highest correlation (r^2 = 0.99, P = 0.003) between activity and sucrose content.

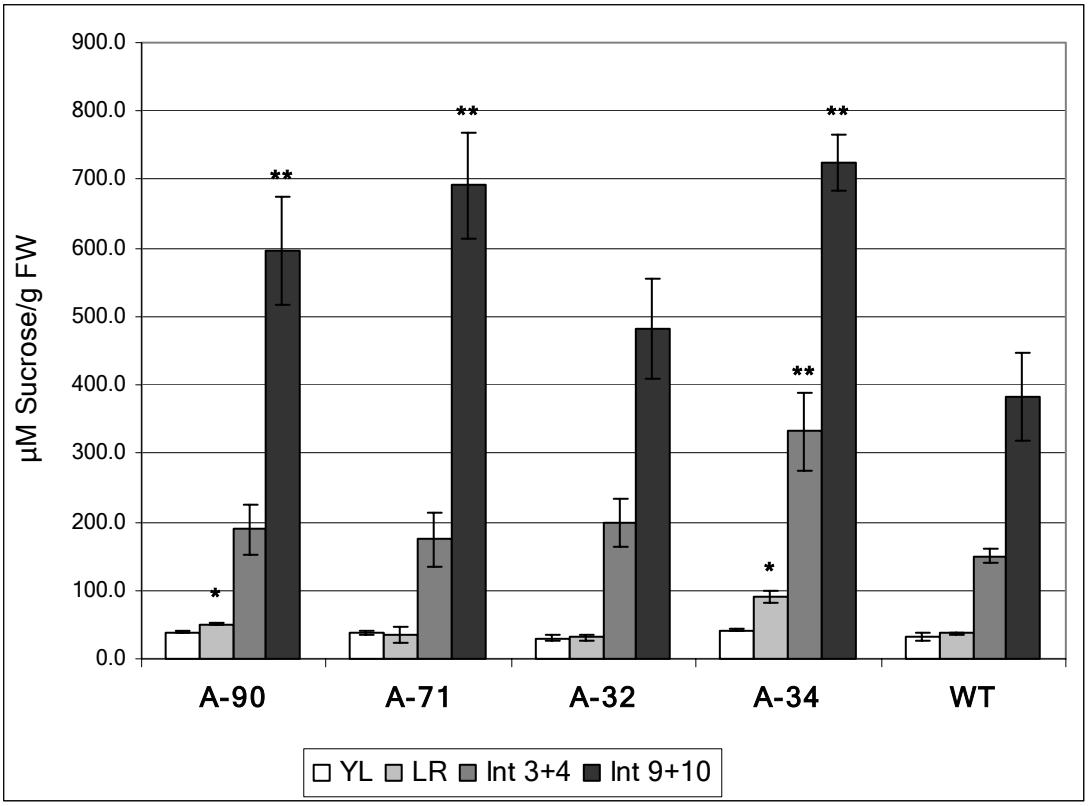

Figure 4.10: Sucrose accumulation in sugarcane with decreased UGD activity.
Sucrose concentration was determined in immature (young leaves, YL and leaf roll, LR), maturing (internode 3+4, I3+4) and mature internodal tissues (internode 9+10, I9+10). Values calculated as mean ± SEM. A-90 – A-34, n = 3; WT, n = 5. * $P \leq 0.1$; ** $P \leq 0.01$

Table 4.1: Glucose accumulation in tissues of sugarcane with antisense repressed *UGD* expression and decreased activity. Values calculated as mean ± SEM and expressed as µM/g FW. A-90 – A-34, n = 3; WT, n = 5. * $P < 0.05$; ** $P < 0.01$

	Young leaf	Leaf roll	Internode 3+4	Internode 9+10
A-90	6.7 ± 1.0	15.0 ± 3.2	4.6 ± 0.5	0.3 ± 0.1
A-71	7.0 ± 2.2	12.9 ± 2.0	20.4 ± 3.5**	2.1 ± 1.1**
A-32	7.1 ± 3.2	17.1 ± 5.1	5.3 ± 1.6	0.4 ± 0.1
A-34	3.4 ± 0.5*	17.1 ± 1.0**	6.4 ± 2.3	1.0 ± 0.3**
WT	3.6 ± 0.7	11.4 ± 1.7	4.3 ± 1.6	0.4 ± 0.1

Glucose (Table 4.1, p39) and fructose (Table 4.2, p.39) concentrations decreased as plant tissue matured indicating that more hexose moieties were being stored as sucrose. Significant differences in glucose and fructose levels are thought to be the result of increased phloem transport after sucrose breakdown in the source tissues.

Table 4.2: Fructose accumulation in tissues of sugarcane with repressed *UGD* expression and decreased activity. Values calculated as mean ± SEM and expressed as µM/g FW. A-90 – A-34, n = 3; WT, n = 5. * $P < 0.05$; ** $P < 0.01$

	Young leaf	Leaf roll	Internode 3+4	Internode 9+10
A-90	0.7 ± 0.1	0.8 ± 0.3	1.0 ± 0.1	1.2 ± 0.1
A-71	0.8 ± 0.1	0.7 ± 0.1*	0.9 ± 0.0	1.4 ± 0.2
A-32	0.8 ± 0.2	0.6 ± 0.1*	1.2 ± 0.1	1.0 ± 0.0
A-34	1.1 ± 0.4	1.0 ± 0.1**	1.1 ± 0.2	0.9 ± 0.1
WT	0.8 ±0.1	0.2 ± 0.0	1.8 ± 0.4	1.2 ± 0.1

4.2.3 SPS activity in young leaves and mature internodes of sugarcane with antisense repressed UGD expression

Sucrose phosphate synthase (Section 1.4.2, p.10-1) is the main sucrose synthesizing enzyme in sugarcane[8] and is its activity is strongly correlated with plant growth-rate and has been shown to increase photosynthesis in tobacco[63]. SPS activity was assayed in both source (Table 4.3, p40) and sink (Table 4.4, p.40) tissues to determine the effect of repressed *UGD* expression on the activity of sucrose synthesizing enzymes. SPS was assayed under V_{lim} and V_{max} conditions to calculate the maximal activity and percentage activation (V_{lim}/V_{max}) in transgenic plants. Statistically significant increases in the activation state of SPS were seen in both source and sink tissues of lines A-90, A-71 and A-32.

Table 4.3: SPS activity in young leaves under limiting (V_{lim}) and maximal (V_{max}) conditions. Activity expressed in nmol/mg protein/min. Mean ± SEM, n = 3, * $P < 0.1$; ** $P < 0.01$.

	V_{max}	V_{lim}	V_{lim}/V_{max}
A-90	134.5 ± 24.4	131.3 ± 1.4	97.6 *
A-71	163.9 ± 17.3	152.9 ± 36.4	93.3 *
A-32	116.7 ± 7.5	116.4 ± 13.3 *	99.8 *
A-34	172.0 ± 19.8	164.1 ± 20.6	95.4
WT	123.4 ± 40.1	96.1 ± 30.1	77.8

Table 4.4: SPS activity in mature internodes under limiting (V_{lim}) and maximal (V_{max}) conditions. Activity expressed in µmol/mg protein/min. Mean ± SEM, n = 3, * $P < 0.1$; ** $P < 0.01$.

	V_{max}	V_{lim}	V_{lim}/V_{max}
A-90	2.2 ± 0.1 *	2.2 ± 0.3	99.7 *
A-71	6.4 ± 1.0 *	5.6 ± 0.5 **	87.0 *
A-32	4.4 ± 0.2 **	3.9 ± 0.5 **	86.9 *
A-34	6.1 ± 1.0 **	5.4 ± 0.8 **	87.9
WT	2.8 ± 0.2	2.3 ± 0.3	80.3

In accordance with previous research on SPS activity in sugarcane conducted in this lab[8], an increase in activity was seen with maturation of the stem in transgenic cane. An activation of 93-99% and 87-99% was shown in the young leaves and mature internodes respectively. Significant increases were also seen in SPS activity under both maximal and limiting conditions in mature tissues. The results indicate a general upregulation of SPS catalyzed sucrose synthesis in transgenic plants.

4.2.4 Sucrose synthase activity in the sucrose synthesis and breakdown direction

Sucrose synthase (Section 1.4.2, p.10-1) is the second enzyme involved in sucrose synthesis in plants. Although SuSy has lower activity than SPS, it is an important accessory sucrose synthesizing enzyme in young immature tissue and also provides UDP-Glc to cellulose synthase through its sucrose breakdown activity in young actively growing tissue. SuSy activity was assayed to determine whether a decrease of the UDP-Glc flux through

UGD had a downstream up-regulating effect on SuSy activity as indicated in SPS (4.2.3, p.39-40).

Table 4.5: SuSy activity in young and mature internodes in the breakdown and synthesis direction. Activity expressed in nmol/mg protein/min. Mean ± SEM, n = 3.

	Sucrose Breakdown		Sucrose Synthesis	
	Young leaf	Int 9+10	Young leaf	Int 9+10
A-90	17.6 ± 8.9	9.5 ± 3.5	1.2 ± 0.5	19.2 ± 3.6
A-71	26.5 ± 9.0	5.0 ± 0.4	0.6 ± 0.2	23.0 ± 1.1
A-32	11.6 ± 8.3	5.9 ± 0.3	1.3 ± 0.1	22.5 ± 2.2
A-34	19.9 ± 0.8	5.5 ± 1.4	0.4 ± 0.1	20.0 ± 2.9
WT	10.8 ± 4.8	6.7 ± 0.8	0.7 ± 0.1	21.7 ± 0.7

SuSy activity (Table 4.5) in the sucrose breakdown direction tended to be higher in immature leaf tissue but increases over WT plants did not reach significance. This increase in sucrose cleavage activity may be due to a compensation taking place to assist with the breakdown of the higher sucrose levels in the source tissues of transgenic plants which have to enter the phloem for transport to the sink tissues. The increase in the breakdown activity of SuSy may also be to provide UDP-Glc to the growing cell wall. SuSy activity was not increased in the sucrose breakdown direction in mature tissue, or in the synthesis direction in immature or mature tissue.

4.2.5 Assay for UDP-glucose pyrophosphorylase activity

UDP-glucose pyrophosphorylase (Section 1.4, p.7-9) reversibly converts UDP-Glc to Glc-1-P. UGPase activity (Figure 4.11, p42) was assayed to determine if the decreased flux of UDP-Glc through UGD in transgenic plants caused an increase in the activity of UGPase in the Glc-1-P synthesis direction due to a larger UDP-Glc 'pool'. UGPase activity was significantly ($P < 0.05$) increased in young tissues of transgenic lines A-90, A-71 and A-34 and also in mature tissue of lines A-32 ($P < 0.01$) and A-34 ($P < 0.05$). This possibly point towards a redirection of carbon flow away from hemicellulose and pectic polymer synthesis from UGD end-products.

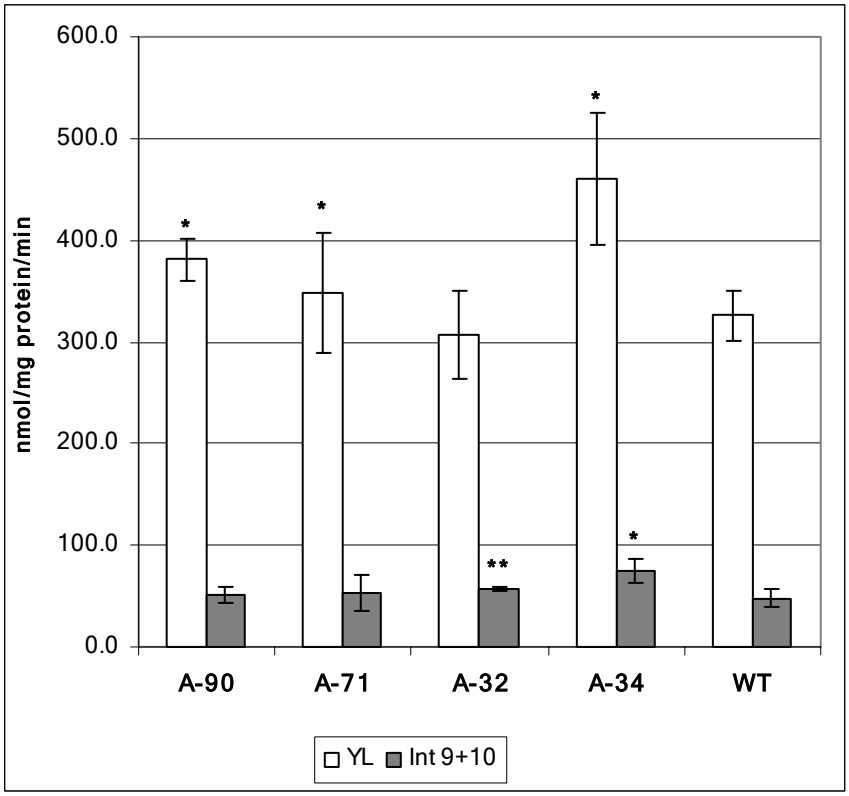

Figure 4.11: UDP-Glucose pyrophosphorylase activity in sugarcane with decreased UGD activity. Values calculated as mean ± SEM. n = 3. * $P \leq 0.05$; ** $P \leq 0.01$.

4.2.6 UDP-Glucose and hexose phosphates in sugarcane with repressed *UGD* expression

UDP-Glc (Section 1.3-4, p.7-9) levels were quantified (Table 4.6, p43) in sugarcane with antisense repressed UGD activity to determine if any changes in the UDP-Glc 'pool' could be detected. UDP-Glc levels were similar in maturing internodes (internode 3+4). Although UDP-Glc in leaf roll was not determined in all transgenic lines, a significant increase (P = 0.04) was shown in line A-34 which also showed strong correlation with decreased UGD activity (r^2 = 0.78) and accumulated the highest levels of sucrose in all internodes.

The metabolites of the hexose phosphate pool were quantified (Table 4.7, p43) to determine if the silencing of UGD and subsequent increases in SPS activation, sucrose accumulation and UGPase activity had any down-stream effect on hexose phosphate metabolism. Glc-6-P was increased in internode 3+4 of transgenic cane and significantly increased in line A-90 (P = 0.007) and A-32 (P = 0.001).

Table 4.6: Hexose phosphates and UDP-Glucose in leaf roll of sugarcane with repressed *UGD* expression and decreased activity. Values calculated as mean ± SEM. A-90 – A-34, n = 3; WT, n = 5. * P ≤ 0.1; ** P ≤ 0.01. Nd = not determined.

	Glucose-6-P (nmol/g FW)	Glucose-1-P (nmol/g FW)	Fructose-6-P (nmol/g FW)	UDP-D-Glucose (pmol/g FW)
A-90 (LR)	0.3 ± 0.01	0.01 ± 0.01	0.05 ± 0.01 *	6.0 ± 1.7
A-71 (LR)	Nd	Nd	Nd	Nd
A-32 (LR)	Nd	Nd	Nd	Nd
A-34 (LR)	0.2 ± 0.05 *	0.01 ± 0.003	0.06 ± 0.02	9.8 ± 1.9 *
WT (LR)	0.3 ± 0.04	0.02 ± 0.004	0.09 ± 0.01	3.1 ± 1.2

Table 4.7: Hexose phosphates and UDP-Glucose in young internodes of sugarcane with repressed *UGD* expression and decreased activity. Values calculated as mean ± SEM. n = 3. * P ≤ 0.1; ** P ≤ 0.01.

	Glucose-6-P (nmol/g FW)	Glucose-1-P (nmol/g FW)	Fructose-6-P (nmol/g FW)	UDP-D-Glucose (pmol/g FW)
A-90 (I3+4)	4.2 ± 0.5 *	1.8 ± 0.7	2.1 ± 0.7	6.9 ± 3.9
A-71 (I3+4)	3.6 ± 0.3 *	0.7 ± 0.04	1.1 ± 0.1	14.2 *
A-32 (I3+4)	4.9 ± 0.5 **	1.0 ± 0.4	1.8 ± 0.1	10.6 ± 3.0
A-34 (I3+4)	2.7 ± 0.2	0.4 ± 0.02	0.8 ± 0.04	4.0 ± 2.0
WT (I3+4)	2.5 ± 0.6	1.1 ± 0.7	1.4 ± 0.5	5.4 ± 1.7

4.3. CELL WALL ANALYSIS

The present project focused on increasing the sucrose accumulation in sugarcane through manipulation of UGD which catalyzes the flux generating reaction providing UDP-GlcA for synthesis of matrix polysaccharides. The cell wall was characterized because of the potential negative effect that silencing of the main pathway for pectin and hemicellulose precursors could have on the structural support of the plant.

4.3.1 Total uronic acid content of cell walls in sugarcane with antisense repressed UGD activity

To determine the effect that silencing of UGD had on the cell wall matrix (Section 1.4.3, p.11-15), alcohol insoluble residues were hydrolyzed and the total uronic component was determined in young, maturing and mature tissues (Figure 4.12). Significant increases in total uronic acids were noted in most of the tissues examined. The increases in uronic acids led to a more in-depth investigation of the cell wall composition and characterization of *myo*-inositol oxygenase expression and activity.

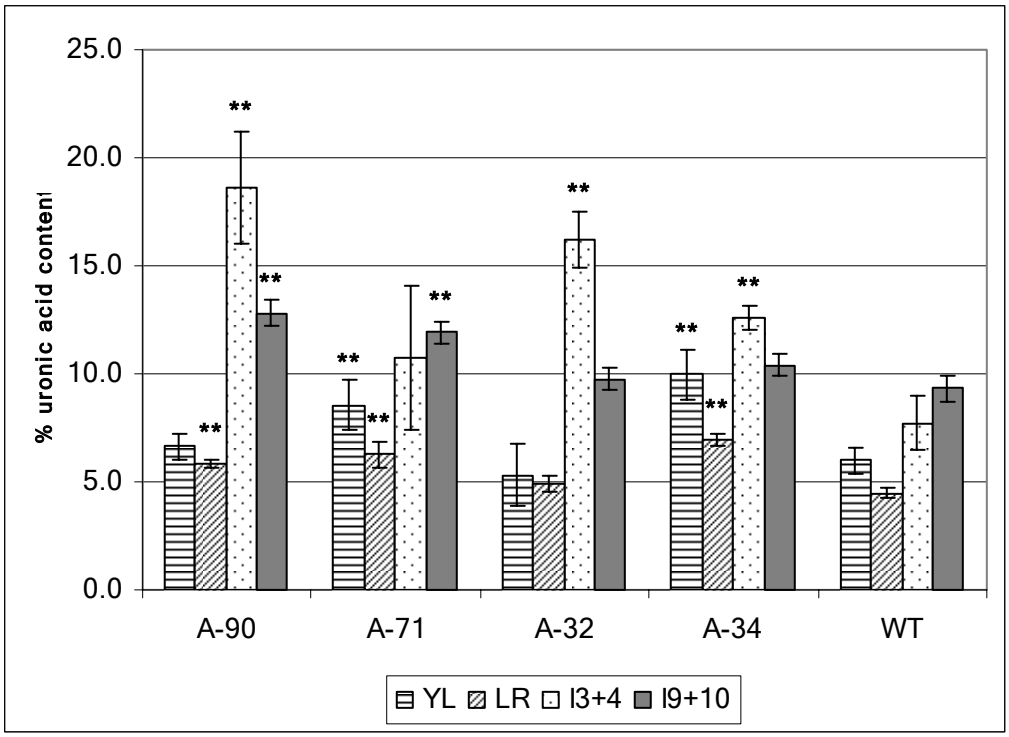

Figure 4.12: Total uronic acid content in cell walls of sugarcane with antisense repressed UGD activity. Values calculated as mean ± SEM. A-90 – A-34, n = 3; WT (wild type), n = 5; ** $P \leq 0.01$.

4.3.2 Total glucose content of cell walls in sugarcane with antisense repressed UGD activity

All of the glucose contained in the cell wall (cellulose, callose and glucans of the cell wall matrix) originates from UDP-Glc. Altered enzyme activities were shown for enzymes surrounding the UDP-Glc 'pool' in transgenic plants and the glucose content of the cell wall (Figure 4.13, 4.14, p.45) was quantified to determine the effect of UGD silencing and the resultant decrease in activity on the structural component of the cell wall. Cell walls were fractionated by enzymatic (AMG) digestion of starch followed by TFA hydrolysis of the non-cellulosic residue and Seaman hydrolysis of the remaining cellulosic residue.

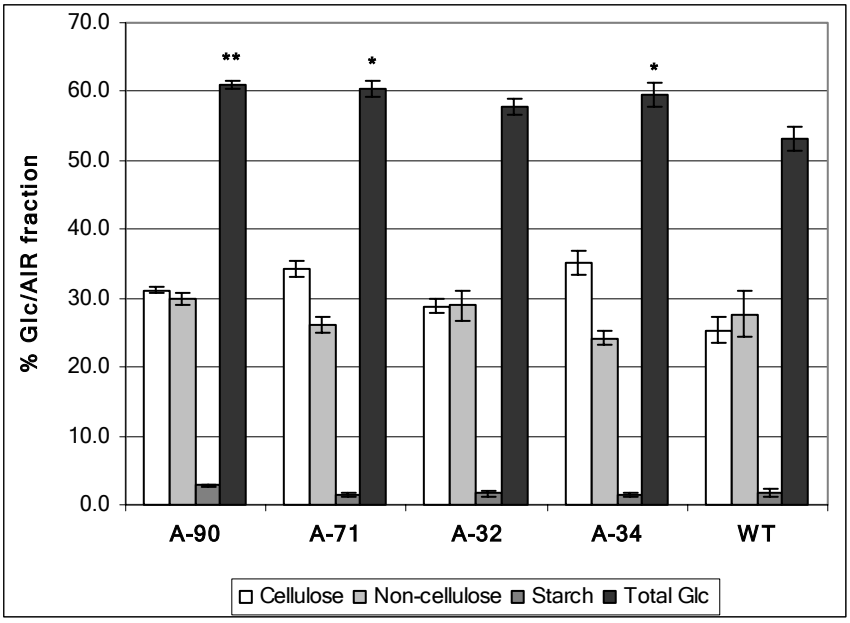

Figure 4.13: Total glucose content of fractionated cell walls in internode 9+10 of sugarcane with antisense repressed UGD activity. Values calculated as mean ± SEM. A-90 - A-34, n = 3; WT (wild type), n = 5; * $P \leq 0.1$, ** $P \leq 0.05$.

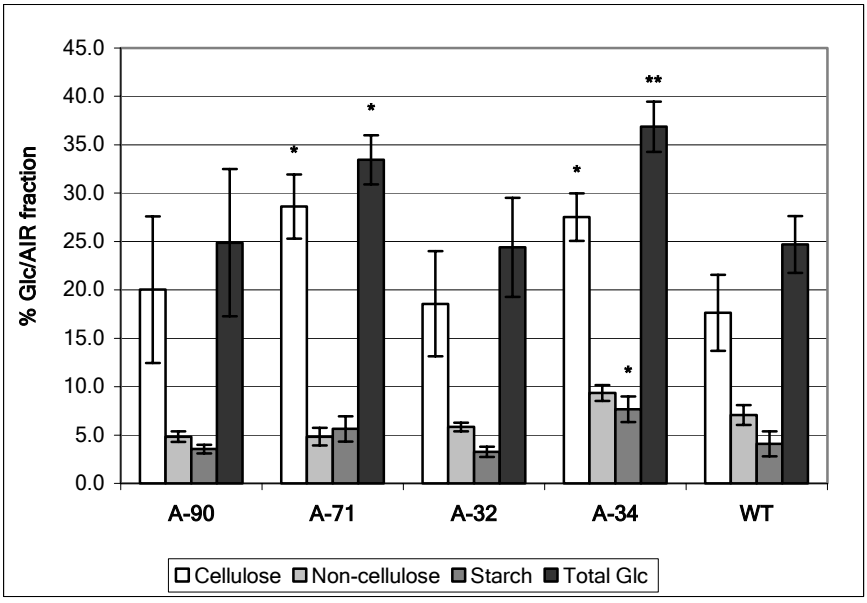

Figure 4.14: Total glucose content of fractionated cell walls in young leaves of sugarcane with antisense repressed UGD activity. Values calculated as mean ± SEM. A-90 - A-34, n = 3; WT (wild type), n = 5; * $P \leq 0.1$, ** $P \leq 0.05$.

The total glucose content of cell walls of mature internodes (Figure 4.13) of transgenic plants were increased in all lines and reached statistical significance in line A-90 ($P = 0.05$), A-71 ($P = 0.08$) and A-34 ($P = 0.1$). Although statistical significance was not shown, all transgenic

lines had increased cellulose fractions. The total glucose content of young leaves (Figure 4.14, p45) was also increased (significant in lines A-71 (P = 0.08) and A-34 (P = 0.03)) in transgenic lines with repressed UGD activity. Young leaves from line A-71 and A-34 had significantly increased cellulose (P = 0.09) and line A-34 (P = 0.1) had significantly increased starch content. The significant increases seen in the glucose content of cell walls indicates that alterations in the UDP-Glc 'pool' made more Glc available for the synthesis of cellulose, callose and other Glc containing matrix polymers.

4.3.3 Monosaccharide content of cell walls in sugarcane with antisense repressed UGD activity

The monosaccharide content of the cell wall was quantified by GC-MS to determine the effect of UGD silencing on the non-cellulosic component (matrix and pectic polymers) of the cell wall (Figure 4.15 and 4.16, p47). Pentose:hexose ratios in mature tissues (internode 9+10) were either unchanged or were slightly increased. Small increases were detected in the Xyl:Gal ratios of transgenic lines A-32 and A-34 in mature internodes, but they were not significant. Ara:Gal ratios were significantly increased in line A-71 (P = 0.04) as well as line A-34 (P = 0.04). Pentose:hexose ratios were unchanged in leaf roll of transgenic lines. The results indicate that the transgenic plants were able to compensate for decreased UGD activity by upregulation of a secondary pathway (the MIOP) for GlcA synthesis and that the MIOP was able to provide all the monomers needed for normal cell wall synthesis. It also points toward less regulation of carbon flux through the MIOP than through UGD which is reflected in increased pentose:hexose ratios.

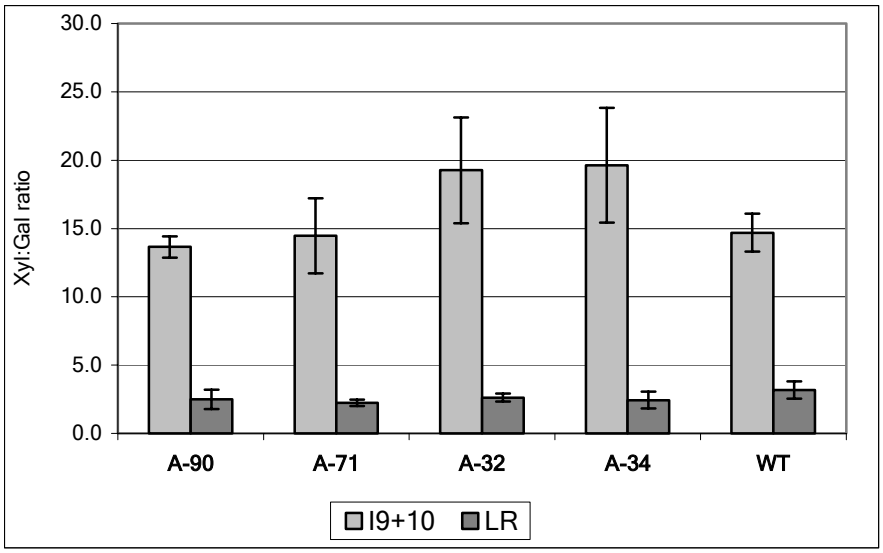

Figure 4.15: Xylose:galactose ratios of cell wall polysaccharide from pAUGdf510 transformed plants. Pentose:hexose ratios of non-cellulosic polysaccharides in the leaf roll (LR) and mature internodes (I9+10) of wild type (WT) and transgenic sugarcane lines. Values are mean ± SEM, A-90 - A-34; n = 3. WT; n = 5. $P \leq 0.05$

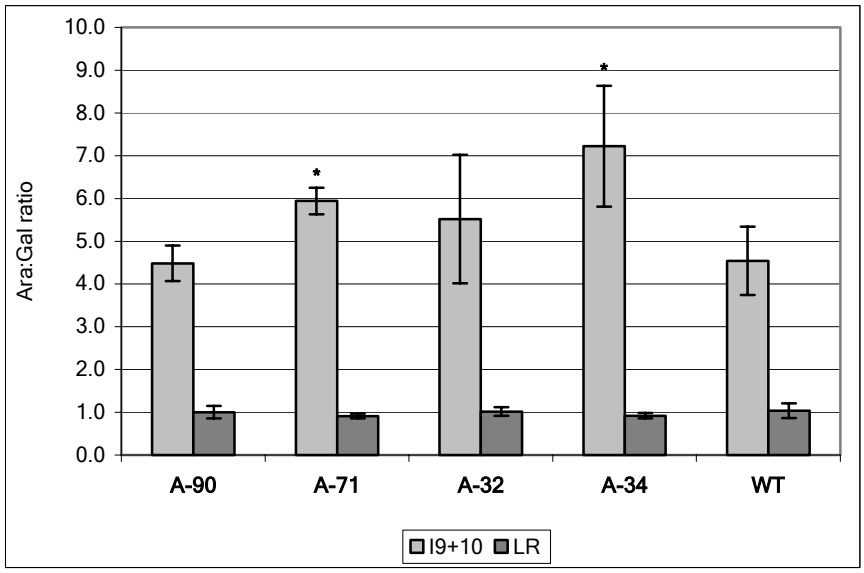

Figure 4.16: Arabinose:galactose ratios of cell wall polysaccharide from pAUGdf510 transformed plants. Pentose:hexose ratios of non-cellulosic polysaccharides in the leaf roll (LR) and mature internodes (I9+10) of wild type (WT) and transgenic sugarcane lines. Values are mean ± SEM, A-90 - A-34; n = 3. WT; n = 5. $P \leq 0.05$

4.3.4 Myo-inositol oxygenase activity in sugarcane with repressed *UGD* expression

It is thought that under conditions where the synthesis of UDP-GlcA through UGD is inhibited, the MIOP will be able to supply the intermediates needed for cell wall synthesis (Section 1.4.3.2, p.12-3). MIOX activity was determined in an attempt to explain the increased levels of uronic acids seen in the transgenic plants with decreased UGD activity. Leaf roll MIOX activity (Figure 4.17, p48) was significantly increased in transgenic line A-34 ($P = 0.04$) and was either similar or slightly increased in the other antisense lines. Leaf roll MIOX activity was increased in all transgenic lines transformed with pHan-UGD and was significantly increased in line H-29 ($P = 0.02$).

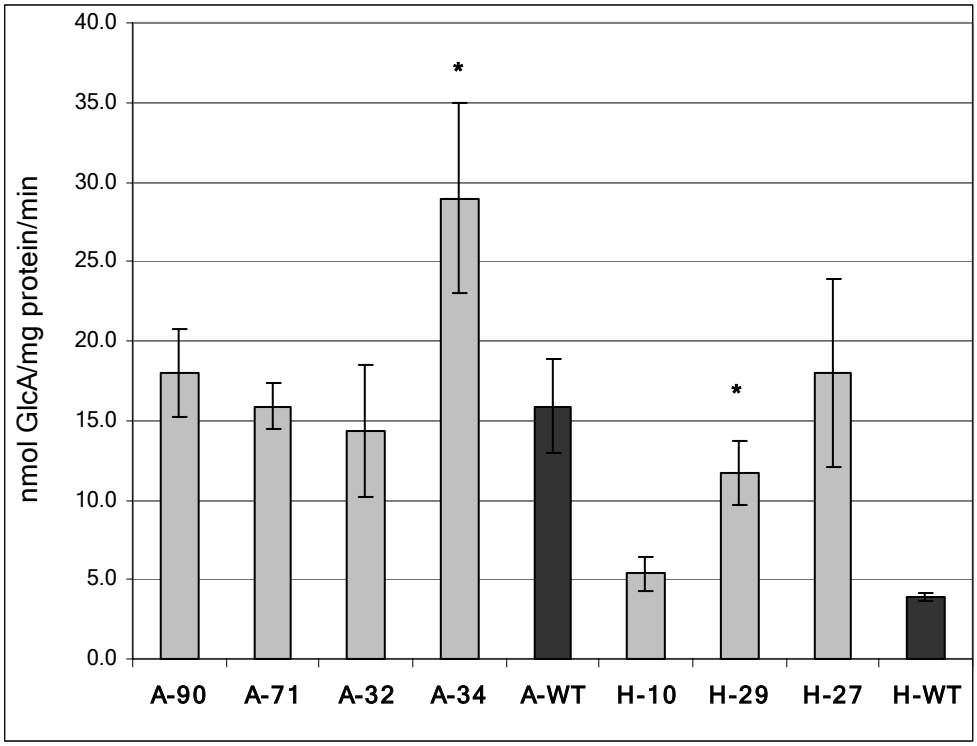

Figure 4.17: Myo-inositol oxygenase activity in the leaf roll of transgenic sugarcane lines with repressed UGD activity. Values calculated as mean ± SEM. 1.1-1A-71, n = 3; WT, n = 5. * $P \leq 0.05$

4.3.5 Semi-quantitative expression analysis of *UGD* and *MIOX* using RT-PCR

One of the possible down-stream effects of silencing *UGD* is that the alternative pathway for synthesis of hemicellulose and pectin precursors, the MIOP, could be up-regulated to supply the necessary nucleotide sugars needed for cell wall synthesis. Semi-quantitative RT-PCR was used to determine if up-regulation of transcripts coding for the first enzyme in the MIOP, namely MIOX did occur in response to the repression of *UGD* transcription. *MIOX* and *UGD* expression were compared in sugarcane lines with decreased *UGD* activity. Results (Figure 4.18, p49) show an increase in *MIOX* transcript levels in young leaves. *MIOX* transcription was also increased in leaf roll (data not shown) and young internodal tissue as a result of antisense repression of endogenous *UGD* transcription.

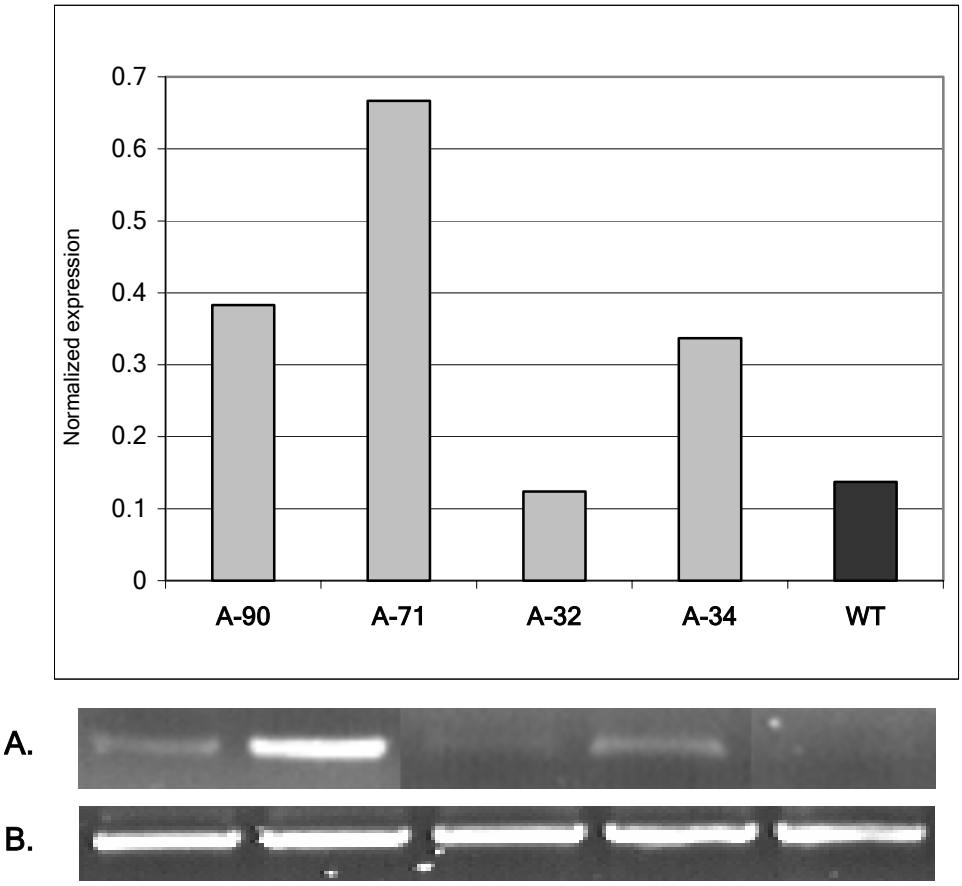

Figure 4.18: Semi-quantitative RT-PCR analysis of *MIOX* expression in immature tissues of transgenic sugarcane with reduced *UGD* activity. **A.** RT-PCR showing levels of *MIOX* transcripts in leaf roll (LR). **B.** α-Actin was used as housekeeping gene to normalize the amount of template cDNA. Five µg total RNA was reverse transcribed using SuperScript III and each PCR reaction contained 0.5 µg cDNA as template. All reactions were as per the manufacturers instructions.

Taken together, the results of the total uronic acid determination (4.3.1, p.44), MIOX activity (4.3.4, p.47-8) and expression analysis of *MIOX* (4.3.5, p.48-9) supports the notion that the MIOP can supply all the cell wall intermediates when UGD activity is suppressed and that the MIOP is not subject to tight feedback inhibition as seen in UGD activity.

4.3.6 Expression analysis of sugarcane *UGD* and *MIOX*

The TIGR-SoGI was searched for *UGD* and *MIOX* EST's using the BLAST algorithm[71]. The reference *UGD* sequence was from sequencing data generated in this lab[41]. A mRNA (AY232552 (miox4)[73]) and three amino acid sequences (NP172904, NP194356, NP200475) for *Arabidopsis MIOX* was obtained from the NCBI nucleotide and protein databases and used in BLAST searches of TIGR-SoGI. Seven libraries were identified having transcripts for both *UGD* (TC56897) and *MIOX* (TC51845). Sugarcane *MIOX* had 66% homology to the *Arabidopsis* sequence and 88% homology to the corresponding sequence of *Zea mays*.

Although four expressed *MIOX* genes have been identified in *Arabidopsis*[30], the present search of TIGR-SoGI did not identify any additional expressed genes in sugarcane. Interestingly, three expressed isoforms of *UGD* was identified (designated *UGD1*, *UGD2* and *UGD3*) with 99%, 96% and 80% sequence homology to the reference sequence.

UGD1 was expressed at the highest level in the apical meristem, developed inflorescence and rachis, leaf roll and seedlings inoculated with *Gluconacetobacter*. In contrast, in low temperature stressed calli, etiolated leaves from *in vitro* grown seedlings and lateral buds, *UGD* and *MIOX* expression were similar. A similar expression pattern for *MIOX* and *UGD* was also found in *Oryza sativa* in a similar experiment.

5. DISCUSSION

Because of the central position of UDP-Glc in carbohydrate metabolism[6], being situated at the branching point of various competing sinks for carbon[74], UGD activity was selected to be manipulated in order to increase the flux of carbon moieties into sucrose. To analyse the effect of decreased UGD on sucrose accumulation in sugarcane, 'antisense' technology and intron-spliced hairpin RNA vectors were constructed and transformed into embryogenic sugarcane calli. Nine sugarcane lines transformed with the antisense vector (pAUGdf510) and four lines transformed with the ihpRNA vector (pHan-UGD) were raised. Northern analysis and RT-PCR indicated that the transformed lines had decreased *UGD* transcript levels and Southern analysis showed that all lines were unique transformation events. Four lines showing antisense repression of *UGD* transcription were chosen for more detailed characterisation.

Although the kinetics[46,48], temporal and spatial distribution of expression and enzyme activity[3] and effects of UGD mutants[33] and overexpression[50] on cell wall composition in higher plants have been studied, the effect of repressed *UGD* expression on sucrose accumulation in plants, to our knowledge, have not been addressed. To determine the effect of repressed *UGD* expression, the enzyme activities and metabolite levels of pathways surrounding the UDP-Glc pool was determined. Even though *UGD* mRNA levels were similar in antisense transformed lines, major differences were shown in enzyme activity between transgenic lines. These differences in enzyme activity without reflection in mRNA levels are explained by experimental data that indicate that transcript levels and enzyme activity does not always correlate[85] and because the relation between transcript level and protein is difficult to predict due to the dependence on how transcript level affects the rate of translation, the rate of protein turnover and on the presence or absence of coordinated regulation of protein degradation.

Transgenic lines that showed significantly decreased UGD activity had significantly increased sucrose accumulation in young, maturing and mature internodes. The increased sucrose accumulation in internode 3 and 4 was highly correlated ($r^2 = 0.99$, $P = 0.003$) with decreased UGD activity in two of the lines (A-32 and A-34) that had the lowest UGD activity. Glucose and fructose concentrations were high in young immature internodes and decreased down the stalk as tissue matured and sucrose storage increased, which is consistent with published data[22,76].

In an attempt to address the increased sucrose accumulation in transgenic lines with decreased UGD enzyme activity, the activity of SPS and SuSy and activation state of SPS was determined in young leaves and in mature storage tissue. It was previously shown that SPS activity increased with maturation of the sugarcane stem, that SPS was the major enzyme responsible for sucrose synthesis in sugarcane and that its activity was highly correlated with sucrose accumulation[8]. Sucrose synthesis is highly regulated and the control occurs mostly at the first step in the pathway which is catalysed by SPS[78]. In agreement with the significant increases seen in sucrose levels, SPS activity in young leaves (source) and mature internodes (sink) in the selected transgenic plants showed significant increases in both activity and activation (V_{lim}/V_{max}) under both V_{max} and V_{lim} (limiting substrate and 5 mM Pi) conditions. In the present study, SPS showed increases in activation of approximately 15-22% in source tissues and 6-19% in sink tissues over control plants.

SuSy activity accounts for less than a quarter of sucrose production in young and maturing sugarcane tissue and is only weakly correlated with sucrose accumulation[8]. Labelling studies by Botha and Black (2000) indicated that sucrose synthesis is exclusively through SPS by internode 9. In the present study, SuSy activity was increased in the young leaves of transgenic lines in the breakdown direction but did not show any changes in either sucrose breakdown in mature tissue or in the synthesis of sucrose in young or mature internodal tissues. The unchanged activities were unexpected as it is thought that the high sucrose content in the mature internodes favours sucrose breakdown[8]. The higher SuSy activity in the breakdown direction in young tissue could be an indication of a sink for carbon import for respiration and biosynthetic activity.

Increasing SPS activity through overexpression was shown to increase sink capacity and sucrose unloading in tomato fruit[77] and also had a positive effect on the overall assimilation and partitioning of carbon into sucrose in tobacco[63]. In addition, significantly increased SPS activity in transgenic tobacco was also accompanied by higher and globally changed sucrose:starch ratios suggesting a major shift in carbohydrate metabolism. In the present study, the significantly increased accumulation of sucrose seen in sugarcane with repressed UGD activity suggests that the sucrose synthesis capacity of transgenic plants and specifically SPS activity or activation was in some way enhanced. It is known that the SPS of immature internodes of sugarcane shows very little sensitivity to Pi inhibition[8] which may be attributed to the SPS activity in these tissues coming mostly from an SPS isoform belonging to the divergent A* sub-family (also named D family[86]) of monocot SPSs in family A that lack the 14-3-3 protein-binding site (Ser_{229}), the Ser residue involved in osmotic stress activation (Ser_{424}) and the ability to be phosphorylated at Ser_{158} which is involved in light-dark

regulation[78]. Recent work by Castledon and co-workers identified five SPS gene families in the Poaceae (grasses)[86]. Three of these form subfamilies homologous to the previously described families A (Family II), B (Family V) and C (Family I) and two form a novel and distinctive family D (D_{III} (Family III) and D_{IV} (Family IV)) which has, to date, only been found in the grasses. The SPS proteins of the D family are smaller (108-109 kDa) than those from the other families (114-119 kDa) and their genes was shown to be constitutively expressed in both the leaves and stem of sugarcane[87] by quantitative real-time PCR (RT-qPCR). Proportionally, the D family of SPS genes are most highly represented in sugarcane stem tissues (up to 50% of total SPS transcripts) and accounts for approximately 20% of the relative expression of SPS in leaves. This suggests that at least some of the SPS activity in sugarcane is not allosterically controlled by Pi inhibition. It is generally accepted that the substrate saturation profiles for both UDP-Glc and Fru-6-P are hyperbolic and that SPS is allosterically activated by Glc-6-P[23]. The levels of Glc-6-P in young internodes of transgenic cane was significantly increased (line A-90 $P = 0.007$, line A-32 $P = 0.001$) over those in control plants and may contribute, to some extent, to the increased activation and subsequent increased sucrose accumulation by increasing the affinity of SPS for both substrates. The increased SPS activity and subsequent increased sucrose levels have the additional effect of stimulating photosynthesis[63], thereby providing more Glc-6-P which has a further activating effect on SPS. Because of the hyperbolic nature of SPS substrate saturation, the increased supply of substrate and activating Glc-6-P by enhanced photosynthesis and the lack of effective feedback inhibition, sucrose synthesis seems to be controlled by substrate levels available to the enzyme.

Studies on enzymes of the nucleotide interconversion pathway revealed that UGD is often the least active enzyme of the pathway leading to the conclusion that UGD might catalyze the rate-limiting step in the production of cell wall hemicellulose and pectin precursors from UDP-Glc[88-90] which, in turn, is also a precursor for cellulose and sucrose synthesis. Transgenic sugarcane lines showed significant increases in sucrose accumulation which was positively correlated with a decrease in UGD activity. Because of the central position of UDP-Glc in the synthesis of various structural polysaccharide components of the cell wall, it was important to determine whether a decrease in UGD activity caused down-stream changes in cell wall composition which could impact on its structural integrity.

40-50% of dry sugarcane bagasse consists of cellulose and 25-35% of hemicelluloses, a heterogeneous polymer mixture composed of Xyl, Ara, Gal, Glc and trace amounts of Man and Rham[79]. The remaining dry weight is made up of approximately 18% lignin, 2-3% ash and 0.8% wax. Total uronic acids (GalA and GlcA) were determined in the present study

because its uridyl-derivatives are the enzymatic products of UGD and of the subsequent 4-epimerization of UDP-GlcA by UGE to UDP-GalA. It was hypothesized that a decrease in carbon flux through UGD would have a negative effect on the pectin and hemicellulose content of transgenic plants. Unexpectedly, uronic acids were significantly increased in young and mature tissues of all transgenic plants. The biosynthesis of cell wall polysaccharides has received much attention in recent years[2,28,80,81]. One of the interesting findings is that plants have two separate pathways for the interconversion of the hexosan and pentosan precursors needed for hemicellulose and pectin synthesis[4,31]. The first pathway is catalysed by UGD which converts UDP-Glc to UDP-GlcA[36]. The second pathway, known as the *myo*-inositol oxygenation pathway, is a three enzyme system which converts *myo*-inositol to UDP-GlcA[32]. Both pathways are temporally and spatially expressed in different tissues and at different developmental stages of *Arabidopsis*[3,30] but the relative contribution of each pathway to matrix polysaccharide synthesis remains unclear.

The increases in uronic acid content of transgenic lines led to a more in-depth investigation of the effect that the down-regulation of UGD had on the expression and activity of the MIOP. A BLAST search using the sequence for *Arabidopsis MIOX* was conducted on the TIGR *Saccharum officinarum* Gene Index to obtain a corresponding sugarcane sequence. The sugarcane sequence had 66% sequence identity to that of *Arabidopsis* and 88% identity to the maize sequence. Sugarcane *MIOX* EST's were found in a total of seven EST libraries including apical meristem, developed inflorescence and rachis, leaf roll and seedlings inoculated with *Gluconacetobacter diazotroficans*. A 'electronic northern' of sugarcane *MIOX* showed expression equal to that of *UGD* in cold stressed calli and leaves and lower expression in leaf roll tissue and lateral buds. This pattern of expression is similar to that shown in *Arabidopsis*[30]. The fact that *UGD* EST's was found in a ratio of approximately 10:1 to *MIOX* EST's indicate that the dominant pathway for cell wall matrix precursor synthesis in sugarcane is through UGD in most instances. Semi-quantitative RT-PCR was used to determine if the antisense repression of *UGD* transcript levels had an effect on the levels of *MIOX* transcripts in young tissues of transgenic sugarcane. Normalized results indicate that *MIOX* transcription increased up to five-fold in transgenic lines over that of wild-type plants. This is the first comparative analysis of *UGD vs. MIOX* mRNA levels in plants with repressed *UGD* transcription and results suggests a degree of 'flexibility' (or plasticity) in the relative contribution of the MIOP and UGD to the pool of cell wall matrix precursors. MIOX activity was increased in both leaf roll and maturing internodes of transgenic lines transformed with antisense and ihpRNA constructs and followed the same trend as those of the *MIOX* transcripts. The increased MIOX activity (up to two-fold in antisense lines and over four-fold in ihpRNA lines) and expression in transgenic lines is an indication that the MIOP was upregulated to compensate for the decrease in carbon flux through UGD.

The two major metabolic effects of decreasing the carbon flux through UGD can either be a flux into cellulose and/or into sucrose. In the present study, total cell wall Glc (cellulosic and non-cellulosic) was determined in destarched cell walls of transgenic plants and showed a significant increase in both young and mature tissues over wild type controls. On further investigation, the increase in total cell wall glucose was shown to be due to a significantly increased cellulose content in transgenic plants which was evident in immature and mature tissues. An increase in sucrose accumulation and an apparent increased activation of SPS was shown in the transgenic plants in the present study. Amor *et al*. (1995) demonstrated that sucrose is the preferred substrate for cellulose synthesis in cotton fibers and it is suggested that the availability of sucrose in the cell affects the rate of cellulose synthesis[17] and can subsequently also be correlated with growth rate[86]. The increase in cell wall Glc in the cellulose fraction in the transgenic plants could thus be a direct effect of the increased sucrose levels supplying more substrate for pSuSy (which is associated with the cellulose synthase complex) at the cell membrane and is further evidence of the redirection of carbohydrate flux away from the hemicellulose and pectin fraction and into the synthetic pathways for cellulose and sucrose. This redirection of flux is also indicated by the significantly increased activity of UGPase in young and mature tissues which was determined in the Glc-1-P synthesizing direction. Although it was hypothesized that an increased availability of Glc-1-P for conversion to ADP-Glc and subsequent increased synthesis of starch could also be possible in transgenic plants, this was not shown in the present study.

Recently, Kärkönen and co-workers demonstrated that in maize UGD mutants the ratio of cell wall pentose:hexose (Xyl:Gal and Ara:Gal) was reduced by only 10% and suggested that either other UGD isozymes or the alternative MIOP was producing the UDP-GlcA necessary for matrix polysaccharide synthesis[33]. To confirm the upregulation of the MIOP in the present study, as was indicated by the increased levels of *MIOX* transcripts and activity and also by the increased total uronic acid content of the matrix polysaccharides of transgenic lines, pentose:hexose ratios were determined by GC-MS. In contrast to the decreased pentose:hexose ratios found in maize mutants, both Xyl:Gal and Ara:Gal ratios were increased in the mature internodes of transgenic plants. This confirms that an upregulation of the MIOP occurred in transgenic lines to compensate for the decrease in UDP-GlcA provided by the antisense repressed UGD activity. It has been suggested that carbon flux through the MIOP is regulated by feedback inhibition of UDP-GlcA and also by substrate inhibition by GlcA-1-P on glucuronokinase[82]. Taking the results of the present study into account, it seems that in sugarcane at least, the activity of the MIOP may not be under the strict regulatory control of its direct or down stream products. The results also indicate a degree of

plasticity in the alternate pathways for UDP-GlcA synthesis which have not been shown before.

6. SUMMARY, CONCLUSION AND FUTURE WORK

In order to understand and manipulate carbon flux to sucrose one needs to consider not only its biosynthetic pathways, but also the competing sinks for carbon in various parts of the plant at different stages of development. UDP-Glc is a central metabolite in the synthesis of both sucrose and most of the cell wall polysaccharides and manipulation of the flux into either of the cell wall components could therefore cause an increase of flux toward one or more of the competing sinks. The present study considers the *in planta* modification of UGD activity which catalyzes the rate limiting step in the biosynthesis of the precursors of both hemicellulose and pectin, a major competing sink for assimilated carbon.

Sugarcane with antisense repressed UGD activity was produced and characterized. Sucrose accumulation was increased in the transgenic lines and was highly correlated with decreased UGD activity. The transgenic lines had increased activation of SPS and in creased UGPase activity in young and mature tissues suggesting an alteration in carbon flux toward sucrose. Because of the importance of a structurally intact cell wall, total cell wall uronic acids and Glc were determined. Both uronic acids and Glc were increased, again suggesting a redirection of carbon. To determine whether the increase in uronic acids could be attributed to upregulation of the MIOP, the expression and activity of the first enzyme of this pathway, MIOX, was determined. Both the expression and activity of MIOX was upregulated in transgenic lines. The increase in cell wall Glc is thought to be a direct effect of higher availability of sucrose to pSuSy which increases the UDP-Glc available to CeS for its synthetic activity. It was shown that the increased cell wall Glc was caused by increases in Glc contained in the cellulose fraction in transgenic plants. Pentose:hexose ratios were also increased in transgenic lines suggesting that cell wall pentoses were still made in adequate amounts for normal synthesis of polysaccharides. The higher levels of uronic acids and pentoses found in the cell wall suggest that the feedback of the MIOP is not as finely modulated as that of UGD.

A simplified hypothetical model for the altered carbon flux in the transgenic sugarcane lines is suggested in Figure 6.1, p54. A decrease of carbon flux toward matrix synthesis in plants with repressed UGD activity increases the cytosolic UDP-Glc pool, thereby providing increased substrate for sucrose synthesis by SPS. The increased sucrose is known to have an activating effect on photosynthesis[63] which, in turn, increases Glc-6-P which has a further

activating effect on SPS. To keep the hexose phosphates in equilibrium, Glc-6-P is converted to Fru-6-P and Glc-1-P (and thus to UDP-Glc by UGPase) which provides further increased substrate levels for SPS. A known effect of increased sucrose accumulation is an increase in cellulose synthesis by CeS. The transgenic lines showed significant increases in cellulose. The cell walls of transgenic plants also showed increased uronic acid and pentose which is attributed to an upregulation of the MIOP which also uses Glc-6-P as substrate.

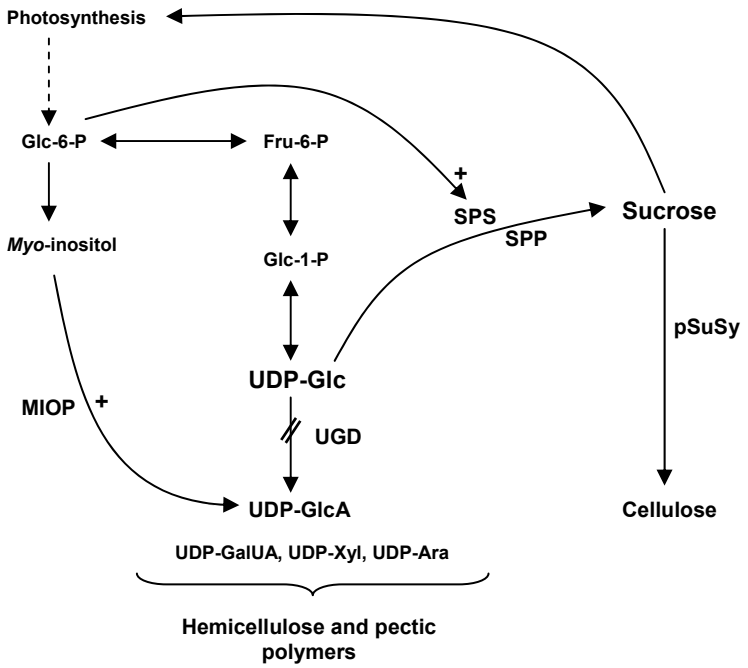

Figure 6.1: Hypothetical model for increased sucrose synthesis in sugarcane with repressed UGD activity.

The exact mechanism for the increased sucrose accumulation in transgenic sugarcane has not been determined. Future work will centre on the characterization of the mechanism and will include GC-MS based metabolite profiling as well as determination of the expression of SPS and SPP. The effectiveness and mechanism of *UGD* repression in increasing sucrose accumulation will also be further investigated in sugarcane where all of the expressed *UGD* genes are co-supressed.

The upregulated MIOP will also be investigated in more detail. The second enzyme of the MIOP, glucuronokinase, will be cloned or purified from the transgenic sugarcane produced for the present study and characterized in a spin-off PhD study. Glucuronate is a precursor of L-ascorbic acid[83]. Another possibility that will be investigated is that L-ascorbic acid could be

produced at higher rates in transgenic lines with an upregulated MIOP because of the increased availability of GlcA.

REFERENCE LIST

1. Grof CPL and Campbell JA. Sugarcane sucrose metabolism: scope for molecular manipulation. *Aust J Plant Physiol* **28**, 1-12. (2001).

2. Cosgrove DJ. Assembly and enlargement of the primary cell wall in plants. *Annu Rev Cell Dev Biol* **13**, 171-201 (1997).

3. Seitz B, Klos C, Wurm M, Tenhaken R. Matrix polysaccharide precursors in Arabidopsis cell walls are synthesized by alternate pathways with organ-specific expression patterns. *Plant J* **21**, 537-46 (2000).

4. Hassid WZ, Neufeld EF, Feingold DS. Sugar nucleotides in the interconversion of carbohydrates in higher plants. *Proc USA Natl Acad Sci* **45**, 905-15 (1959).

5. Leloir LF. The enzymatic conversion of uridine diphosphate glucose into a galactose derivative. *Arch Biochem Biophys* **33**, 186-90 (1951).

6. Kleczkowski LA, Geisler M, Ciereszko I, Johansson H. UDP-Glucose pyrophosphorylase. An old protein with new tricks. *Physiol Plant* **134**, 8. (2004).

7. Feingold DS. Encyclopedia of plant physiology. Loewus FA and Tanner W. (ed.) (Springer-Verlag, Berlin,1982).

8. Botha FC and Black KG. Sucrose phosphate synthase and sucrose synthase activity during maturation of internodal tissue in sugarcane. *Aust J Plant Physiol* **27**, 81-5 (2000).

9. Muñoz P, Norambuena L, Orellana A. Evidence for a UDP-Glucose transporter in Golgi-aparatus derived vesicles from pea and its possible role in polysaccharide biosynthesis. *Plant Physiol* **112**, 1585-1594. (1996).

10. Gibeaut DM. Nucleotide sugars and glycosyltransferases for synthesis of cell wall matrix polysaccharides. *Plant Physiol Biochem* **38**, 69-80 (2000).

11. Buchanan BB, Gruissem W, Jones RL. Biochemistry & molecular biology of plants. John Wiley & Sons Ltd., West Sussex, UK. (2002).

12. Fry SC. The growing plant cell wall: chemical and metabolic analysis. Blackburn Press, Cadwell, New Jersey (2000).

13. Reiter W-D. Biosynthesis and properties of the plant cell wall. *Curr Opin Plant Biol* **5**, 536-42 (2002).

14. Keegstra K and Raikhel N. Plant glycosyltransferases. *Curr Opin Plant Biol* **4**, 219-24 (2001).

15. Amor Y, Haigler CH, Johnson S, Wainscott M, Delmer DP. A membrane-associated form of sucrose synthase and its potential role in synthesis of cellulose and callose in plants. *Proc Natl Acad Sci USA* **92**, 9353-7 (1995).

16. Kutschera U and Heiderich A. Sucrose metabolism and cellulose biosynthesis in sunflower hypocotyls. *Physiol Plant* **114**, 372-9. (2002).

17. Babb VM and Haigler CH. Sucrose phosphate synthase activity rises in correlation with high-rate cellulose synthesis in three heterotrophic systems. *Plant Physiol* **127**, 1234-42. (2001).

18. Arioli T, Peng L, Betzner AS, Burn J, Wittke W, Herth W, *et al*. Molecular analysis of cellulose biosynthesis in *Arabidopsis* . *Science* **279**, 717-20 (1998).

19. Sato S, Kato T, Kakegawa K, Ishii T, Liu Y-W, Awano T, *et al*. Role of the putative membrane-bound *endo*.1,4-β-D-glucanase KORRIGAN in cell elongation and cellulose synthesis in *Arabidopsis thaliana*. *Plant Cell Physiol* **42**, 251-63 (2001).

20. Haq S and Hassid WZ. Biosynthesis of sucrose phosphate with sugarcane leaf chloroplasts. *Plant Physiol* **40**, 591-4 (1965).

21. Echeverria E, Salvucci ME, Gonzalez P, Paris G, Salerno G. Physical and kinetic evidence for an association between sucrose-phosphate synthase and sucrose-phosphate phosphatase. *Plant Physiol.* **115**, 223-7 (1997).

22. Moore PH. Temporal and spatial regulation of sucrose accumulation in the sugarcane stem. *Aust J Plant Physiol* **22**, 661-79 (1995).

23. Huber SC and Huber JL. Role and regulation of sucrose-phosphate synthase in higher plants. *Annu Rev Plant Physiol Plant Mol Biol* **47**, 431-44. (1996).

24. Roberts RM. The formation of uridine diphosphate-glucuronic acid in plants. Uridine diphosphate-glucuronic acid pyrophosphorylase from barley seedlings. *J Biol Chem* **246**, 4995-5002 (1971).

25. Strominger JL, Mapson LW. Uridine diphosphoglucose dehydrogenase of pea seedlings. *Biochem J* **66**, 567 (1957).

26. Reiter WD, Vanzin GF. Molecular genetics of nucleotide sugar interconversion pathways in plants . *Plant Mol Biol.* **47**, 95-113 (2001).

27. Charalampous FC and Lyras C. Biochemical studies on inositol. IV. Conversion of inositol to glucuronic acid by rat kidney extracts. *J Biol Chem* **228**, 1-13 (1957).

28. Carpita NC. Structure and biogenesis of the cell walls of grasses. *Annu Rev Plant Physiol Plant Mol Biol* **47**, 445-76. (1996).

29. Kotake T, Yamaguchi D, Ohzono H, Hojo S, Kaneko S, Ishida H, Tsumuraya Y. UDP-sugar pyrophosphorylase with broad substrate specificity: toward various monosaccharide 1-phosphates from pea sprouts. *J Biol Chem* **279**, 45728-36 (2004).

30. Kanter U, Usadel B, Guerineau F, Li Y, Pauly M, Tenhaken R. The inositol oxygenase gene family of Arabidopsis is involved in the biosynthesis of nucleotide sugar precursors for cell-wall matrix polysaccharides. *Planta* **221(2)**, 243-54 (2005).

31. Loewus FA. Carbohydrate interconversions. *Ann Rev Plant Physiol* **22**, 337-64 (1971).

32. Loewus FA, Kelly S, Neufeld EF. Metabolism of myo-insitol in plants: conversion to pectin, hemicellulose, D-xylose, and sugar acids. *Proc USA Nat Acad Sci* **48**, 421-25 (1962).

33. Kärkönen A, Murigneux A, Martinant J-P, Pepey E, Tatout C, Dudley BJ, Fry SC. UDP-Glucose dehydrogenase of maize-a role in cell wall pentose biosynthesis. *Biochem J* **391(Pt 2)** 409-15 (2005).

34. Griffith CL, Klutts JS, Zhang L, Levery SB, Doering TL. UDP-glucose dehydrogenase plays multiple roles in the biology of the pathogenic fungus *Cryptococcus neoformans*. *J Biol Chem* **279**, 51669-76 (2004).

35. Loewus FA and Loewus MW. *myo*-Inositol: Its biosynthesis and metabolism. *Ann Rev Plant Physiol* **83**, 137-61 (1983).

36. Strominger JL, Kalchar HM, Axelrod J, Maxwell ES. Enzymatic oxidation of uridine diphosphate glucose to uridine diphosphate glucuronic acid. *J Am Chem Soc* **76**, 6411-2 (1954).

37. Ge X, Penney LC, van de Rijn I, Tanner ME. Active site residues and mechanism of UDP-glucose dehydrogenase. *Eur J Biochem* **271**, 14-22 (2004).

38. Ridley WP, Houchins JP, Kirkwood S. Mechanism of action of uridine diphosphoglucose dehydrogenase. *J Biol Chem* **250**, 8761-7 (1975).

39. Bdolah A and Feingold DS. Uridine diphosphate D-glucose dehydrogenase of *Aerobacter aerogenes*. *J Bacteriol* **96**, 1144-9 (1968).

40. Loewus F, Chen MS, Loewus ML. Biogenesis of plant cell wall polysaccharides. F Loewus (ed.), pp. 1-28 (**Academic Press, New York**,1983).

41. Van der Merwe J. The characterization of the UDP-glucose dehydrogenase gene and regulatory sequences of sugarcane. PhD Thesis/Dissertation, University of Stellenbosch (2005).

42. Johansson H, Sterky F, Amimi B, Lundeberg J, Kleczkowski LA. Molecular cloning and characterization of a cDNA encoding poplar UDP-glucose dehydrogenase, a key gene of hemicellulose/pectin formation. *Biochim Biophys Acta* **1576**, 53-8 (2002).

43. Tenhaken R and Thulke O. Cloning of an enzyme that synthesizes a key nucleotide-sugar precursor of hemicellulose biosynthesis from soybean: UDP-glucose dehydrogenase. *Plant Physiol* **112**, 1127-34 (1996).

44. Hinterberg B, Klos C, Tenhaken R. Recombinant UDP-glucose dehydrogenase from soybean. *Plant Physiol Biochem* **40**, 1011-17 (2002).

45. Stewart DC and Copeland L. Uridine 5'-diphosphate-glucose dehydrogenase from soybean nodules. *Plant Physiol* **116**, 349-55 (1998).

46. Steward DC and Copeland L. Kinetic properties of UDP-glucose dehydrogenase from soybean nodules. *Plant Science* **147**, 119-25 (1999).

47. Robertson D, Smith C, Bolwell GP. Inducible UDP-glucose dehydrogenase from French bean (Phaseolus vugaris L.) locates to vascular tissue and has alcohol dehydrogenase activity. *Biochem J* **313**, 311-7 (1996).

48. Turner W and Botha FC. Purification and kinetic properties of UDP-glucose dehydrogenase from sugarcane. *Arch Biochem Biophys* **407**, 209-16 (2002).

49. Kärkönen A and Fry SC. Novel characteristics of UDP-glucose dehydrogenase activities in maize: non-involvement of alcohol dehydrogenase in cell wall polysaccharide biosynthesis. *Planta* **223(4)**, 858-70 (2006).

50. Samac DA, Litterer L, Temple G, Jung HJ, Somers DA. Expression of UDP-glucose dehydrogenase reduces cell-wall polysaccharide concentration and increases xylose content in alfalfa stems. *Appl Biochem Biotechnol* **113-116**, 1167-82 (2004).

51. Mullis K, Faloona F, Scharf S, Saiki R, Horn G, Erlich H. Specific enzymatic amplification of DNA *in vitro*: the polymerase chain reaction. *Cold Spring Harb Symp Quant Biol* **51**, 263-73 (1986).

52. Wesley VS, Helliwel CA, Smith NA, Wang MB, Rouse DT, Liu Q, *et al*. Construct design for efficient, effective and high-throughput gene silencing in plants. *Plant J* **27**, 581-90 (2001).

53. Sambrook J, Fritsch EF, Maniatis T. Molecular Cloning: A Laboratory Manual. Cold Spring Harbour Laboratory Press, Cold Spring Harbour, NY (1989).

54. Bower R, Elliott AR, Potier BAM, Birch RG. High-efficiency, microprojectile mediated co-transformation of sugarcane, using visible or selectable markers. *Molec Breed* **2**, 239-49 (1996).

55. Birch RG and Bower R. Particle Bombardment Technology for Gene Transfer. Yang NS and Christou P eds (ed.), pp. 3-37 (Oxford University Press, New York,1994).

56. Murashige T and Skoog F. A revised medium for rapid growth and bioassays with tobacco tissue cultures. *Physiol Plant* **15**, 97. (1962).

57. McGarvey P and Kaper JM. A simple and rapid method for screening transgenic plants using the PCR. *Biotechniques* **11**, 428-32 (1991).

58. Dellaporta SL, Wood J, Hicks JB. A plant DNA minipreparation. *Plant Mol Biol Reporter* **1**, 19-21 (1983).

59. Innis MA, Myambo KB, Gelfand DH, Brow MA. DNA sequencing with *Thermus aquaticus* DNA polymerase and direct sequencing of polymerase chain reaction-amplified DNA. *Proc Nat Acad Sci USA* **85**, 9436-40 (1988).

60. Bugos RC, Chiang VL, Zhang XH, Campbell ER, Podila GK, Campbell WH. RNA isolation from plant tissues recalcitrant to extraction in guanidine. *Biotechniques* **19**, 734-7 (1995).

61. Laemmli UK. Cleavage of structural proteins during assembly of the head of bacteriophage T4. *Nature* **227**, 680-7. (1970).

62. Bergmeyer HU and Bernt E. Methods of enzymatic analysis. Bergmeyer HU (ed.), pp. 1176-9 (**Verlag Chemie Weinheim Academic Press**, New York,1974).

63. Baxter CJ, Foyer CH, Turner J, Rolfe SA, Quick WP. Elevated sucrose-phosphate synthase activity in transgenic tobacco sustains photosynthesis in older leaves and alters development. *J Exp Bot* **54**, 1813-20 (2003).

64. Stitt M,Lilley RM, Gerhardt R, Heldt HW. Metabolite levels in specific cells and subcellular compartments of plant leaves. *Methods Enzymol* **174**, 518-52 (1989).

65. Räbina J, Maki M, Savilahti EM, Jarvinen N, Penttila L, Renkonen R. Analysis of nucleotide sugars from cell lysates by ion-pair solid-phase extraction and reversed-phase high-performance liquid chromatography. *Glycoconj J.* **18**, 799-805. (2001).

66. Bradford MM. Rapid and qualitative method for quantification of microgram quantities of protein utilising the principle protein-dye binding. *Anal Biochem.* **72**, 248-52. (1976).

67. Blumenkrantz N and Asboe-Hansen G. New method for quantitative determination of uronic acids. *Anal Biochem* **54**, 484-89 (1973).

68. van den Hoogen BM, van Weeren PR, Lopez-Cardonzo M, van Golde LMG, Barneveld A, van de Lest CHA. A microtiter plate assay for the determination of uronic acids. *Anal Biochem.* **257**, 107-11 (1998).

69. Reddy CC, Swan JS, Hamilton GA. myo-Inositol oxygenase from hog kidney. I. Purification and characterization of the oxygenase and of an enzyme complex containing the oxygenase and D-glucuronate reductase. *J Biol Chem* **256**, 8510-8. (1981).

70. Arner RJ, Prabhu KS, Reddy CC. Molecular cloning, expression , and characterization of myo-inositol oxygenase from mouse, rat, and human kidney. *Biochem Biophys Res Commun* **4**, 1386-92. (2004).

71. Altschul SF, Gish W, Miller W, Myers EW, Lipman DJ. Basic local alignment search tool. *J Mol Biol* **215**, 403-10. (1990).

72. Roessner U, Wagner C, Kopka J, Trethewey RN, Willmitzer L. Simultaneous analysis of metabolites in potato tuber by gas chromatography-mass spectrometry. *Plant J* **23**, 131-42 (2000).

73. Lorence A, Chevone BI, Mendes P, Nessler CL. Myo-inositol oxygenase offers a possible entry into plant ascorbate biosynthesis. *Plant Physiol* **134**, 1200-5 (2004).

74. Delmer DP and Haigler CH. The regulation of metabolic flux to cellulose, a major sink for carbon in plants. *Metabolic Engineering* **4**, 22-8. (2002).

75. Moore PH, Botha FC, Furbank RT, Grof CPL. Intensive sugarcane production: meeting the challenges beyond 2000. Keegstra K and Raikhel N (ed.), pp. 141-55 (CAB International, Wallingford,1997).

76. Whittaker A and Botha FC. Carbon partitioning during sucrose accumulation in sugarcane internodal tissue. *Plant Physiol* **115**, 1651-9. (1997).

77. Nguyen-Quoc B, N'Tchobo H, Foyer CH, Yelle S. Overexpression of sucrose-phosphate synthase increases sucrose unloading in transgenic tomato fruit. *J Exp Bot* **50**, 785-91. (1999).

78. Lunn JE and MacRae E. New complexities in the synthesis of sucrose. *Curr Opin Plant Biol* **6**, 208-14 (2003).

79. Sun JX, Sun XF, Sun RC, Su YQ. Fractional extraction and structural characterization of sugarcane bagasse hemicelluloses. *Carb Polymer* **56**, 195-204 (2004).

80. Chapple C and Carpita N. Plant cell walls as targets for biotechnology. *Curr Opin Plant Biol* **1**, 179-85. (1998).

81. Bolwell GP. Biosynthesis of plant cell wall polysaccharides. *Trends Glycoscience Glycotechnol* **12**, 143-60 (2000).

82. Leibowitz MD, Dickinson DB, Loewus FA, Loewus M. Partial purification and study of pollen glucuronokinase. *Arch Biochem Biophys* **179**, 559-64 (1977).

83. Lorence A, Chevone BI, Mendes P, Nessler CL. *Myo*-inositol oxygenase offers a possible entry point into plant ascorbate biosynthesis. *Plant Physiol* **134**, 1200-5 (2004).

84. Schäfer WE,Rohwer JM,Botha FC. A kinetic study of sugarcane sucrose synthase. *Eur J Biochem* **271**, 3971-7 (2004).

85. Gibon Y, Blaesing OE, Hannemann J, Carillo P, Höhne M, Hendriks JHM, *et al*. A Robot-based platform to measure multiple enzyme activities in Arabidopsis using a set of cycling assays: Comparison of changes of enzyme activities and transcript

levels during diurnal cycles and in prolonged darkness. *The Plant Cell* **16**, 3304-25 (Dec 2004).

86. Castledon CK, Aoki N, Gillespie VJ, MacRae EA, Quick WP, Buchner P, *et al*. Evolution and function of the sucrose-phosphate synthase gene families in wheat and other grasses. *Plant Physiol* **135**, 1573-64 (2004).

87. Grof CPL, So CTE, Perroux JM, Bonnet GD, Forrester RI. The five families of sucrose-phosphate synthase genes in *Saccharum* spp. are differentially expressed in leaves and stem. *Functional Plant Biol* **33**, 605-10 (2006).

88. Amino S, Takeuchi Y, Komamine A. Change in the enzyme activities involved in formation and interconversion of UDP-sugars during cell cycle in a synchronous culture of *Catharanthus roseus*. *Physiol Plant* **64**, 110-7 (1985).

89. Dalessandro D, Northcote DH. Changes in enzymatic activities of nucleoside diphosphate sugar interconversions during differentiation of cambium to xylem in sycamore and poplar. *Biochem J* **162**, 267-79 (1977).

90. Dalessandro D, Northcote DH. Possible control sites of polysaccharide synthesis during cell growth and wall expansion of pea seedlings (*Pisum sativum* L.). *Planta* **134**, 39-44 (1977).

ACKNOWLEDGEMENT

I would like to express my sincerest gratitude to:

Professor Jens Kossmann for guidance and for assistance in the proofreading of this manuscript.

Professor Frikkie Botha for initiating this project.

My parents, Piet and Isabelle Bekker, for their patience, love and support and for giving me the means and opportunity to become whatever I want to be.

Staff and students of the Institute for Plant Biotechnology, University of Stellenbosch.

Fletcher Hiten, Charmaine Stander and Hennie Groenewald for always being available to listen and to exchange ideas.

Professor Jacqui Greenberg, Human Genetics, University of Cape Town.